Block-Biased Mamba for Long-Range Sequence Processing

Annan Yu
Center for Applied Mathematics
Cornell University
Ithaca, NY 14853
ay262@cornell.edu

N. Benjamin Erichson
Lawrence Berkeley National Laboratory
International Computer Science Institute
Berkeley, CA 94720
erichson@icsi.berkeley.edu

Abstract

Mamba extends earlier state space models (SSMs) by introducing input-dependent dynamics, and has demonstrated strong empirical performance across a range of domains, including language modeling, computer vision, and foundation models. However, a surprising weakness remains: despite being built on architectures designed for long-range dependencies, Mamba performs poorly on long-range sequential tasks. Understanding and addressing this gap is important for improving Mamba's universality and versatility. In this work, we analyze Mamba's limitations through three perspectives: expressiveness, inductive bias, and training stability. Our theoretical results show how Mamba falls short in each of these aspects compared to earlier SSMs such as S4D. To address these issues, we propose B_2S_6, a simple extension of Mamba's S6 unit that combines block-wise selective dynamics with a channel-specific bias. We prove that these changes equip the model with a better-suited inductive bias and improve its expressiveness and stability. Empirically, B_2S_6 outperforms S4 and S4D on Long-Range Arena (LRA) tasks while maintaining Mamba's performance on language modeling benchmarks.

1 Introduction

Mamba [25] has recently emerged as an exciting alternative to Transformers, demonstrating strong empirical performance not only in language tasks [84, 45], but also in a variety of domains, including vision [107, 103], audio [43], time series forecasting [43], and operator learning [33]. Based on the state-space model (SSM) framework of S4 and S4D, Mamba replaces attention with a selective state space mechanism. Unlike attention, which computes pairwise interactions across the sequence, this approach uses data-dependent weights in a recurrent structure, aligning with the temporal nature of sequential data. Despite its success as a general-purpose sequence modeling tool [51], Mamba consistently underperforms on benchmarks such as the Long-Range Arena (LRA) [3]. This limitation is surprising, given that Mamba is derived from architectures specifically designed for modeling long-range dependencies. This behavior raises an important question:

Why does Mamba struggle with long-range sequence modeling?

To address this question, we conduct a theoretical analysis of the S6 state-space unit that underlies the Mamba architecture. Our goal is twofold: first, to explain why Mamba underperforms on long-range sequence tasks, and second, to provide a principled remedy. Through a rigorous mathematical analysis, we identify three key factors that limit Mamba's ability to model long-range dependencies:

- **Expressiveness.** Unlike S4D, which allows each internal channel to learn an independent recurrent unit, Mamba shares parameters across all channels. Therefore, one should not interpret Mamba as

39th Conference on Neural Information Processing Systems (NeurIPS 2025).

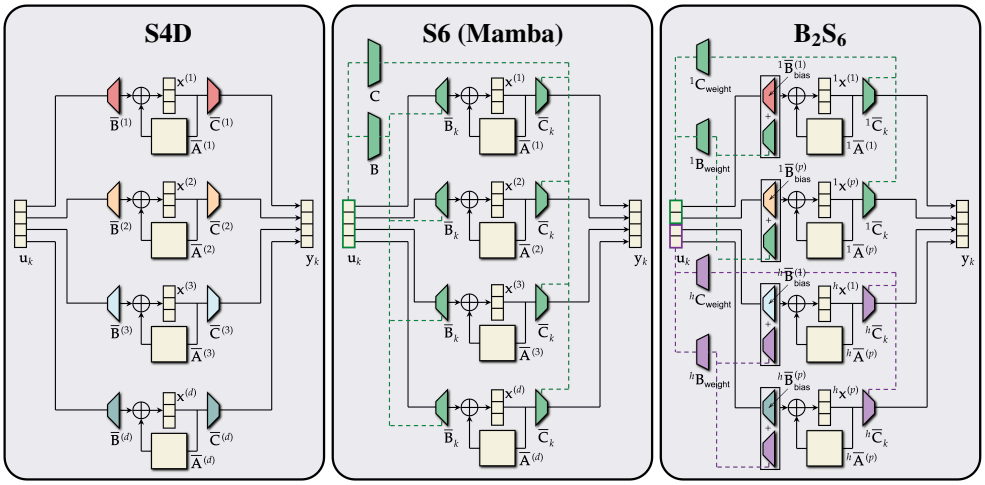

Figure 1: Comparison of S4D, S6, and B_2S_6 units. S4D uses independent linear SSM units for each channel, giving it high capacity (or width) but no input-dependent selectivity. S6 introduces a selective mechanism that modulates its internal dynamics based on the input, but shares parameters across channels, limiting its effective width and expressiveness. Our proposed B_2S_6 unit partitions the input into smaller blocks, enabling selective behavior across multiple subspaces (see also [20]). Additionally, it includes a channel-specific, input-independent bias term that further increases model capacity. These design choices improve the performance on long-range sequence tasks.

a straightforward extension of S4D that gains time-variant benefits at no cost. Rather, Theorem 1 shows that while Mamba introduces input-dependent dynamics, it also sacrifices certain degrees of freedom. Most notably, it has a weaker ability to learn independent behavior in each channel.

- **Inductive Bias.** Unlike S4D, which uses a position-based bias that helps preserve long-range memory, Mamba adaptively decides what information to remember or forget based on the input. This input-dependent mechanism is too extreme and can cause the model to discard useful long-term information too quickly, leading to poor retention in long-range tasks (see Theorem 2).
- **Training Stability.** Unlike S4D, which tends to train reliably on long sequences, Mamba empirically exhibits unstable training behavior on the LRA benchmark tasks. We theoretically show that this instability comes from the input-dependent selection mechanism, which becomes increasingly difficult to optimize as the length of the sequence increases (see Theorem 3).

Motivated by these findings, we propose the *Block-Biased-S6* unit (B_2S_6), a simple yet principled extension of the S6 architecture that addresses its limitations in modeling long-range dependencies (see Figure 1). Like S6, B_2S_6 retains the selective mechanism that modulates internal dynamics based on the input. However, instead of computing the selection weights from the full input $\mathbf{u}_k$, we divide the model into smaller blocks, with each block operating on a subset of $\mathbf{u}_k$. This multihead structure was already suggested in [20], but in addition to that, we introduce an input-independent, channel-specific bias term to the recurrent unit (see Table 1). We prove that these modifications enhance B_2S_6's expressiveness and assign it a more appropriate inductive bias for handling long-range dependencies. We also apply a reduced learning rate to the parameters governing the input-dependent sampling intervals, which improves training stability. Together, these modifications enable B_2S_6 to model long-range dependencies more effectively. On the LRA benchmark, B_2S_6 resurrects Mamba from failure and even outperforms S4 and S4D. Furthermore, we show that B_2S_6 achieves comparable perplexity to Mamba when trained on language tasks, demonstrating its versatility across domains.

Contributions. Our main contributions are as follows:

1. We analyze the limitations of Mamba in modeling long-range dependencies and provide theoretical results that characterize the failure modes from three key aspects: (i) expressiveness (see Theorem 1), (ii) inductive bias (see Theorem 2), and (iii) training stability (see Theorem 3).
2. We introduce the B_2S_6 unit, a principled extension of the S6 architecture. We show that B_2S_6 has universal approximation capabilities (see Theorem 4) and is thus more expressive, while also equipped with a more suitable inductive bias for long-range sequence processing (see Theorem 5).

Table 1: A comparison of different classes of selective or non-selective state space models.

	S4D	S5	Mamba	Mamba2	B2S6
Δ_t Dependency	input-independent	input-independent	input-dependent	input-dependent	input-dependent
B/C Dependency	input-independent	input-independent	input-dependent	input-dependent	both
Number of Heads	≥ 1	≥ 1	$= 1$	≥ 1	≥ 1
Parameters	complex	complex	real	real	complex
Parameterization of $\mathbf{A}$	diagonal	diagonal	diagonal	scalar	diagonal

3. We evaluate B_2S_6 on the Long-Range Arena benchmark, where it achieves state-of-the-art performance. In addition, a preliminary examination on the SlimPajama dataset [78] shows that B_2S_6 matches Mamba's performance on language modeling tasks, demonstrating its versatility.

2 The S4D and S6 recurrent units

Introduced in [28] and [27], the S4 and S4D recurrent units process sequences of d-dimensional inputs $\mathbf{u} = (\mathbf{u}_1, \ldots, \mathbf{u}_L)$ to produce corresponding d-dimensional outputs $\Gamma_{\text{S4/S4D}}(\mathbf{u}) = \mathbf{y} = (\mathbf{y}_1, \ldots, \mathbf{y}_L)$. Throughout this paper, we use subscripts to index positions in a sequence and superscripts to index channels. For example, $\mathbf{u}_k^{(i)}$ denotes the ith entry of the kth input vector $\mathbf{u}_k$. Each channel of the S4/S4D model is computed independently with a linear system. For the ith channel, the update rule is

$$\mathbf{x}_k^{(i)} = \overline{\mathbf{A}}^{(i)}\mathbf{x}_{k-1}^{(i)} + \overline{\mathbf{B}}^{(i)}\mathbf{u}_k^{(i)}, \quad \mathbf{y}_k^{(i)} = \overline{\mathbf{C}}^{(i)}\mathbf{x}_k^{(i)}, \qquad 1 \leq i \leq d, \tag{1}$$

where $\mathbf{x}_k^{(i)} \in \mathbb{C}^{n\times 1}$ is the hidden state with initial condition $\mathbf{x}_0^{(i)} = \mathbf{0}$, and $\mathbf{u}_k^{(i)} \in \mathbb{R}$. The matrices $\overline{\mathbf{A}}^{(i)} \in \mathbb{C}^{n\times n}$, $\overline{\mathbf{B}}^{(i)} \in \mathbb{C}^{n\times 1}$, and $\overline{\mathbf{C}}^{(i)} = \mathbb{C}^{1\times n}$ are derived from a continuous-time system. While there are many different discretization rules, we focus on the Zero-Order Hold (ZOH) discretization:

$$\overline{\mathbf{A}}^{(i)} = \exp(\Delta^{(i)}\mathbf{A}), \quad \Delta^{(i)} = \exp(b^{(i)}), \qquad \overline{\mathbf{B}}^{(i)} = \mathbf{A}^{-1}(\overline{\mathbf{A}}^{(i)} - \mathbf{I})\mathbf{B}^{(i)}, \quad \overline{\mathbf{C}}^{(i)} = \mathbf{C}^{(i)}. \tag{2}$$

Here, $\mathbf{A} \in \mathbb{C}^{n\times n}$, $\mathbf{B}^{(i)} \in \mathbb{C}^{n\times 1}$, $\mathbf{C}^{(i)} \in \mathbb{C}^{1\times n}$, and $b^{(i)} \in \mathbb{R}$ are trainable parameters, specific to each channel $1 \leq i \leq d$.[1] S4 and S4D are particularly well-suited for modeling sequences with long-range dependencies and achieve state-of-the-art results on the Long-Range Arena benchmark. This strength is largely due to the reparameterized $\Delta^{(i)}$ values, which, when chosen small, give the model long-term memory by slowing the system dynamics. S4 and S4D differ only in how the matrix $\mathbf{A}$ is represented; we henceforth focus on S4D, which uses a diagonal $\mathbf{A}$ consistent with Mamba.

One limitation of the S4D units is that their dynamics are linear and time-invariant. The S6 units [25] used in the Mamba models improve upon this by making the dynamics input-dependent. More specifically, given a d-dimensional input sequence $\mathbf{u} = (\mathbf{u}_1, \ldots, \mathbf{u}_L)$, an S6 unit computes the ith channel of the output $\Gamma_{\text{S6}}(\mathbf{u}) = \mathbf{y} = (\mathbf{y}_1, \ldots, \mathbf{y}_L)$ as follows:

$$\mathbf{x}_k^{(i)} = \overline{\mathbf{A}}_k^{(i)}\mathbf{x}_{k-1}^{(i)} + \overline{\mathbf{B}}_k^{(i)}\mathbf{u}_k^{(i)}, \quad \mathbf{y}_k^{(i)} = \overline{\mathbf{C}}_k\mathbf{x}_k^{(i)}, \qquad 1 \leq i \leq d, \tag{3}$$

where $\mathbf{x}_k^{(i)} \in \mathbb{R}^n$ and $\mathbf{u}_k^{(i)}, \mathbf{y}_k^{(i)} \in \mathbb{R}$. The matrices $\overline{\mathbf{A}}_k^{(i)}$, $\overline{\mathbf{B}}_k^{(i)}$, and $\overline{\mathbf{C}}_k$ are computed at each step as

$$\overline{\mathbf{A}}_k^{(i)} = \exp(\Delta_k^{(i)}\mathbf{A}), \quad \Delta_k^{(i)} = \text{softplus}(\mathbf{w}^\top\mathbf{u}_k + b^{(i)}), \quad \overline{\mathbf{B}}_k^{(i)} = \mathbf{A}^{-1}(\overline{\mathbf{A}}_k^{(i)} - \mathbf{I})\mathbf{B}\mathbf{u}_k, \quad \overline{\mathbf{C}}_k = \mathbf{u}_k^\top\mathbf{C}. \tag{4}$$

The trainable parameters of the model are $\mathbf{A} \in \mathbb{R}^{n\times n}$, $\mathbf{B} \in \mathbb{R}^{n\times d}$, $\mathbf{C} \in \mathbb{R}^{d\times n}$, $\mathbf{w} \in \mathbb{R}^d$, and $b^{(i)} \in \mathbb{R}$ for all $1 \leq i \leq d$.[2] The key innovation in the S6 architecture lies in the input-dependent dynamics. Both $\overline{\mathbf{B}}_k$ and $\overline{\mathbf{C}}_k$ change with each input step, introducing nonlinearity into the system. In addition, the sampling interval $\Delta^{(i)}$ is also input-dependent, allowing the model to vary the rate at which it memorizes or forgets information. Comparing eq. (4) to eq. (2), we note that $\mathbf{B}\mathbf{u}_k$ and $\mathbf{u}_k^\top\mathbf{C}$ in an S6 are shared across all channels, while $\mathbf{B}^{(i)}$ and $\mathbf{C}^{(i)}$ in an S4D are channel-specific. In the next section, we show how this distinction limits the "effective width" and expressiveness of an S6 unit.

[1] Note that we tie the matrix $\mathbf{A}$ across all channels, which is consistent with the LRA training setup. This choice can be loosened without affecting the essence of the paper.

[2] In many implementations of Mamba, the selection of $\Delta_k^{(i)}$ is more complex, and $\overline{\mathbf{B}}_k$ may be computed using a forward Euler method instead. We follow the formulation in Algorithm 2 of the original Mamba paper [25].

3 A single-layer Mamba is not a universal approximator

A universal approximation theorem (UAT) characterizes the expressive power of neural networks by showing that, under certain conditions, they can approximate any target function to arbitrary accuracy, provided they are sufficiently wide or deep [60, 39]. While UATs do not directly address training dynamics, they serve as a useful sanity check for a model's theoretical capacity. For deep S4D models, some universal approximation results have been established in [87]. In this section, we prove a new UAT of S4D and a new non-UAT of S6 that highlight how the shared state matrices in S6 significantly constrain its expressiveness. We investigate the task of learning a univariate sequential task defined by a ground-truth function G, using a single-layer model that takes in an input $(u_1, \dots, u_L)$, linearly embeds the input into a d-dimensional space, passes it through an S4D or S6 unit, and then decodes the output. More precisely, we consider the class of models (see Figure 5) defined by

$$\tilde{G}(\mathbf{u}) = \tilde{G}((u_1, \dots, u_L)) = \mathbf{N}\sigma(\Gamma((\mathbf{M}u_1, \dots, \mathbf{M}u_L))_L + \boldsymbol{\theta}), \tag{5}$$

where $\mathbf{M} \in \mathbb{R}^{d\times 1}$ is an encoder, $\mathbf{N} \in \mathbb{R}^{d\times 1}$ is a decoder, $\boldsymbol{\theta} \in \mathbb{R}^{d\times 1}$ is a bias term, and $\sigma : \mathbb{R} \to \mathbb{R}$ is a nonlinear activation function applied entrywise to the last output of an S4D or S6 unit Γ. There is only one remaining issue: in the definition of S6, we have $\overline{\mathbf{C}}_k = u_k^\top \mathbf{C}$. That means $\Gamma_{\text{S6}}((\mathbf{M}u_1, \dots, \mathbf{M}u_L))_L$ is zero as long as $u_L = 0$, which makes $\tilde{G}$ with Γ_{S6} clearly not universal approximators on the domain $[0, 1]^L$. To avoid "cheating" in this way, we assume that $u_L = 1$ and only focus on approximating functions on $[0, 1]^{L-1} \times \{1\}$, which makes our non-UAT stronger.

Theorem 1. The single-layer S4D models are universal approximators of continuous functions, but the single-layer S6 models are not. More precisely, fixing a constant for $\Delta^{(i)}$ for all $1 \le i \le d$ in eq. (2) and $\Delta_k^{(i)}$ for all $1 \le i \le d$ and $1 \le k \le L$ in eq. (4), the following two statements hold:

1. Let $\sigma : \mathbb{R} \to \mathbb{R}$ be any Lipschitz continuous, non-polynomial activation function. Given any continuous function $G : [0, 1]^L \to \mathbb{R}$ and any $\epsilon > 0$. There exist some $d \ge 1$, $n \ge 1$, and a choice of parameters $\mathbf{M}, \mathbf{N}, \boldsymbol{\theta}, \mathbf{A}, \mathbf{B}^{(i)}$, and $\mathbf{C}^{(i)}$, where $1 \le i \le d$, such that the map $\tilde{G}$ in eq. (5) with $\Gamma = \Gamma_{\text{S4D}}$ in eq. (1) satisfies that $|\tilde{G}(\mathbf{u}) - G(\mathbf{u})| \le \epsilon$ for any $\mathbf{u} \in [0, 1]^L$.

2. Let $\sigma : \mathbb{R} \to \mathbb{R}$ be any function and let $L \ge 3$ be given. There exists a continuous function $G : [0, 1]^{L-1} \times \{1\} \to \mathbb{R}$ and some $\epsilon > 0$ such that for any $d \ge 1$, any $n \ge 1$, and any choice of parameters $\mathbf{M}, \mathbf{N}, \boldsymbol{\theta}, \mathbf{A}, \mathbf{B}$, and $\mathbf{C}$, the map $\tilde{G}$ in eq. (5) with $\Gamma = \Gamma_{\text{S6}}$ in eq. (3) satisfies that $|\tilde{G}(\mathbf{u}) - G(\mathbf{u})| > \epsilon$ for some $\mathbf{u} \in [0, 1]^{L-1} \times \{1\}$.

You should not interpret Theorem 1 as a pessimistic claim that Mamba models are incapable of solving complex tasks. In practice, Mamba architectures typically use multiple stacked layers and do not fix $\Delta_k^{(i)}$, both of which enhance the expressiveness. Rather, it highlights that an S6 unit is not a simple extension of S4D that inherits all of its structural principles, and the sharing of the $\mathbf{B}$ and $\mathbf{C}$ matrices across all channels can reduce its capacity, making it potentially less effective than S4D for certain tasks. Beyond its impact on approximation capacity, this also leads to issues in larger models, such as training instability [23, 16, 67], reduced generalization [5, 92, 11, 100, 40], and challenges in interpretability [104, 94].

While Theorem 1 assumes that Δ is fixed, we use a synthetic experiment to demonstrate that even when Δ is trainable, the channel-independent design of $\mathbf{B}$ and $\mathbf{C}$ in S6 limits its ability to solve certain problems than S4D. Consider the input function $u(t; \boldsymbol{g}) = \sum_{i=1}^{10} g_i \cos(p_i t)$, where $p_1, \dots, p_{10}$ are the 10 smallest prime numbers and $\boldsymbol{g} \in \mathbb{R}^{10}$ is a coefficient vector. The learning task is to recover $\boldsymbol{g}$ from the function $u(t; \boldsymbol{g})$, i.e., to learn the mapping $G : u(t; \boldsymbol{g}) \mapsto \boldsymbol{g}$. Intuitively, if the model is sufficiently wide, each channel can specialize in capturing one of the cosine components, making the problem easy. We train both a single-layer S6 model and a single-layer S4D model to approximate this mapping, also allowing the Δ-related parameters to be learned in both cases. As shown in Figure 2, the performance of the S6 model remains nearly constant as the width d increases, reflecting the fact that its effective width does not scale with d. In contrast, the S4D model benefits significantly from increased width.

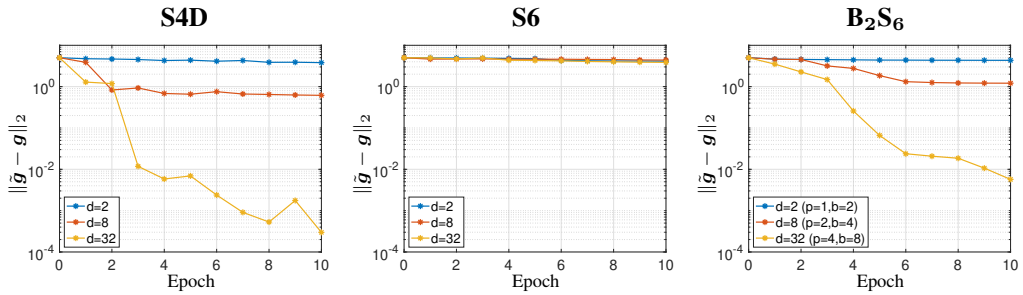

Figure 2: The mean loss $\|\tilde{\boldsymbol{g}} - \boldsymbol{g}\|_2$ between the true coefficient $\boldsymbol{g}$ and the model prediction $\tilde{\boldsymbol{g}}$. Every model has a single layer and is trained for 10 epochs. Here, d is the number of channels in a model. For the $\mathrm{B_2S_6}$ model, h is the number of blocks and p is the number of channels in each block.

4 Mambas exhibit strong inductive bias

A necessary condition for a model to obtain the capability of handling long-range dependency is that it possesses long-term memory. In S4D models, this is achieved by learning small values of $\Delta^{(i)}$, which slow down the evolution of the continuous-time LTI systems and allow information to persist over longer time horizons [74]. In contrast, S6 models introduce an input-dependent sampling interval $\Delta_k^{(i)}$, where certain inputs lead to larger values of $\Delta_k^{(i)}$, causing faster memory decay, while others result in smaller values and slower decay.

This input-adaptive memory control serves as a useful inductive bias in language modeling, where only a limited number of words in a sentence typically carry semantic significance. However, this same mechanism is less suitable for many LRA tasks involving non-linguistic sequences, such as `Image`, `Pathfinder`, and `PathX`, where inputs are derived from flattened pixel arrays. In these settings, while some positional bias may exist (e.g., central pixels may be more informative than peripheral ones), it is difficult to justify that pixels of certain colors in a CIFAR image should receive dramatically more attention than others. As a result, the input-dependent memory dynamics of S6 may act as an overly aggressive or misaligned inductive bias in such contexts.

To formalize the notion of input-dependent bias, let Γ denote either an S4D or S6 unit as defined in eq. (1) and eq. (3), respectively. Given a d-dimensional input sequence $\mathbf{u} = (\mathbf{u}_1, \ldots, \mathbf{u}_L)$, we ask: how does the output of Γ depend on each individual input vector $\mathbf{u}_k$? To study this, we examine the relative gradient of the output with respect to each $\mathbf{u}_k$. Specifically, we define:

$$S_k = \frac{\|\mathbf{J}_k\|_F}{\sum_{k'=1}^{L} \|\mathbf{J}_{k'}\|_F}, \qquad \mathbf{J}_{k'} = \frac{\partial}{\partial \mathbf{u}_{k'}} \Gamma(\mathbf{u}_1, \ldots, \mathbf{u}_L)_L \in \mathbb{R}^{d \times d}, \tag{6}$$

where $\|\cdot\|_F$ denotes the Frobenius norm, and $\mathbf{J}_{k'}$ is the Jacobian of the final output vector with respect to the k'-th input vector. Intuitively, the quantity S_k measures the relative influence of $\mathbf{u}_k$ on the final output. In other words, it tells us how much of the output's sensitivity to perturbations is attributed to the k-th input. For a linear system such as S4D, the Jacobians $\mathbf{J}_{k'}$ are independent of the input $\mathbf{u}$, so the relative gradients S_k remain constant across different inputs. This indicates that the model treats all inputs uniformly and does not introduce bias toward a particular input *as* $\mathbf{u}$ *changes*. In contrast, we now show that S6 units introduce a bias when input vectors vary in magnitude.

Theorem 2. An S6 unit imposes an exponentially large bias as the input magnitude increases. That is, fix a $k_0 \leq L$ and let $\mathbf{A} \in \mathbb{R}^{n \times n}$ be a diagonal matrix with negative diagonal entries and $\mathbf{w} \neq \mathbf{0}$. For almost every (a.e.) input sequence $\mathbf{u} = (\mathbf{u}_1, \ldots, \mathbf{u}_L) \in \mathbb{R}^L$ and a.e. parameters $\mathbf{B} \in \mathbb{R}^{n \times d}$, $\mathbf{C} \in \mathbb{R}^{d \times n}$, and $\mathbf{b} \in \mathbb{R}^d$, let $S_{\mathrm{S6},k}$ be defined in eq. (6), where $\Gamma = \Gamma_{\mathrm{S6}}$ is defined in eq. (3). As $c \to \infty$, the following statements hold for any $p > 0$:

1. If $\mathbf{w}^\top \mathbf{u}_{k_0} > 0$, we have

$$S_{\mathrm{S6},\,k}((\mathbf{u}_1, \ldots, \mathbf{u}_{k_0-1}, c\mathbf{u}_{k_0}, \mathbf{u}_{k_0+1}, \ldots, \mathbf{u}_L)) = \begin{cases} \mathcal{O}(c^{-p}) & , \; k < k_0, \\ \Theta(c^{-1}) & , \; k = k_0, \\ \Theta(1) & , \; k > k_0. \end{cases}$$

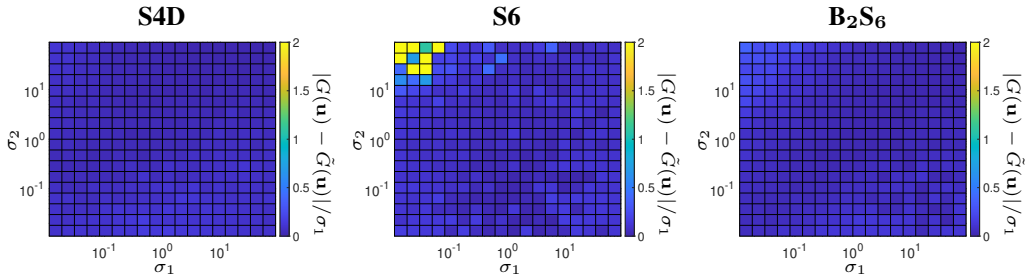

Figure 3: The mean relative loss $|G(\mathbf{u}) - \tilde{G}(\mathbf{u})|/\sigma_1$ for different choices of σ_1 and σ_2. The S6 model cannot make useful predictions when σ_1 is small and σ_2 is large; B_2S_6 fixes this. In all experiments, we fix $d = 32$. For B_2S_6, we set $h = 8$ and $p = 4$.

2. If $\mathbf{w}^\top \mathbf{u}_{k_0} < 0$, we have

$$S_{\text{S6},\,k}((\mathbf{u}_1, \ldots, \mathbf{u}_{k_0-1}, c\mathbf{u}_{k_0}, \mathbf{u}_{k_0+1}, \ldots, \mathbf{u}_L)) = \begin{cases} \Theta(1) & , \ k \neq k_0, \\ \mathcal{O}(c^{-p}) & , \ k = k_0. \end{cases}$$

Moreover, let $S_{\text{S4D},k}$ be defined in eq. (6), where $\Gamma = \Gamma_{\text{S4D}}$ is defined in eq. (1). We have that $S_{\text{S4D},k}$ is constant and does not depend on the input $\mathbf{u}$.

The theorem shows that as the magnitude of a single input vector $\mathbf{u}_{k_0}$ grows, one of two extreme behaviors can emerge: either the current input (Case 2) or all previous inputs (Case 1) exert an exponentially diminishing influence on the final output. Neither outcome is desirable when modeling sequences with long-range dependencies. In practice, many implementations of Mamba mitigate this issue through normalization layers that constrain the magnitudes of input vectors. Additionally, unlike the original formulation in [25], more sophisticated parameterizations are often used to compute the sampling intervals $\Delta_k^{(i)}$. These modifications can be interpreted as efforts to counteract the exponential input bias introduced by large-magnitude vectors.

From Theorem 2, we see another perspective of the limitation of S6: in the computation of $\Delta_k^{(i)} = \text{softplus}(\mathbf{w}^\top \mathbf{u}_k + b^{(i)})$, the vector $\mathbf{w}$ defines two half-spaces in $\mathbb{R}^d$. Inputs $\mathbf{u}_k$ that lie in the positive half-space produce larger values of Δ, leading to slower dynamics and better memorization, whereas those in the negative half-space yield smaller Δ, resulting in faster forgetting. This setup restricts the model's ability to assign distinct memorization biases to different nonlinear regions of the input space. In section 6, we will see how B2S6 improves upon this.

To illustrate the inductive bias of S6, we consider a synthetic task with inputs sampled from

$$\mathbf{u} = (\mathbf{u}_1, \mathbf{0}, \ldots, \mathbf{0}, \mathbf{u}_L), \qquad \mathbf{u}_1 = [u_1, \ldots, u_1]^\top \in \mathbb{R}^d, \quad u_1 \sim \mathcal{N}(0, \sigma_1), \quad \mathbf{u}_L \sim \mathcal{N}(\mathbf{0}, \sigma_2 \mathbf{I}_d),$$

where $\sigma_1, \sigma_2 > 0$ are fixed. The task is to learn the mapping $G(\mathbf{u}) = |u_1|$. Since the target size scales with σ_1, we report the relative error $|G(\mathbf{u}) - \tilde{G}(\mathbf{u})|/\sigma_1$ to make comparisons fair across different settings. Figure 3 shows the relative errors of different models under different values of σ_1 and σ_2. While the S4D model remains robust across all cases, the S6 model fails significantly when σ_1 is small and σ_2 is large. This corroborates Theorem 2: a large input $\mathbf{u}_L$ in the half-space $\{\mathbf{u} \mid \mathbf{w}^\top \mathbf{u} > 0\}$ triggers fast forgetting, erasing the memory of $\mathbf{u}_1$ and making the prediction unreliable.

5 Mambas are not stable to train

Our discussion so far has focused on the expressiveness and generalization of S6 models. In general, a model lacking expressiveness cannot achieve low training error on complex tasks, while poor generalization refers to models that fit the training data well but perform poorly on test data. If you have trained S6 models on LRA tasks, then you might observe another issue: the training loss curve does not decrease smoothly. Occasionally, a single optimization step causes the model to collapse, turning a high-accuracy model into one that performs no better than random guessing. This reflects a training stability issue rather than one of expressiveness or generalization.

This phenomenon has been empirically studied in the context of general neural networks [21, 19], where instability is often linked to sharp curvature in the loss landscape. In this section, we provide

a theoretical explanation for the training instability observed in S6 models. Since we are not tied to a specific task or loss function, we instead study how the output $\Gamma(\mathbf{u};\mathbf{\Theta})$ depends on the model parameters $\mathbf{\Theta}$. While curvature involves second-order derivatives, we focus on first-order gradients. If $(\partial/\partial\mathbf{\Theta})\Gamma(\mathbf{u};\mathbf{\Theta})$ is large in magnitude, large curvatures in the loss landscape might appear when we compose $\Gamma(\mathbf{u};\mathbf{\Theta})$ with other functions to form a loss function.

We find that instability in S6 models is closely tied to how the sampling interval Δ is computed. To formalize this, we prove a theorem comparing the gradients of S6 and S4D models with respect to their Δ-related parameters. For simplicity, we restrict our analysis to a single-input setting, i.e., $d = 1$, and drop all superscripts. Hence, the $\Delta^{(1)}$ for S4D in eq. (2) only depends on a parameter $b = b^{(1)} \in \mathbb{R}$ and the $\Delta_k^{(1)}$ for S6 in eq. (4) only depends on two parameters $w \in \mathbb{R}$ and $b = b^{(1)} \in \mathbb{R}$. Since the specific input distribution is unknown, we make a generic assumption that the inputs are random variables with mild regularity conditions, ensuring that the analysis is broadly applicable.

Theorem 3. Assume that $d = 1$ and $n \geq 1$. Let $\Gamma_{\text{S4D}}(\mathbf{u};\mathbf{\Theta})$ and $\Gamma_{\text{S6}}(\mathbf{u};\mathbf{\Theta})$ be given in eq. (1) and (3), respectively, where $\mathbf{\Theta}$ is the collection of all model parameters. Given a diagonal matrix $\mathbf{A} \in \mathbb{R}^{n\times n}$ whose diagonal entries are negative, and $\mathbf{B} \in \mathbb{R}^{n\times 1}$, the following statements hold:

1. An S6 model is less stable to train than an S4D model as the input magnitude increases. That is, fix some $L \geq 1$, $b \in \mathbb{R}$, and $w = 0$. Let $\mathbf{u} = (u_1, \ldots, u_L)$ be sampled from a distribution $\mathbb{D}$. For every $\mathbf{C} \in \mathbb{R}^{1\times n}$, if $\mathbb{E}_{\mathbf{u}\sim\mathbb{D}_L}|(\partial/\partial w)\Gamma_{\text{S6}}|$, $\mathbb{E}_{\mathbf{u}\sim\mathbb{D}_L}|(\partial/\partial b)\Gamma_{\text{S6}}|$, $\mathbb{E}_{\mathbf{u}\sim\mathbb{D}_L}|(\partial/\partial b)\Gamma_{\text{S4D}}| \neq 0$, then
$$\frac{\mathbb{E}_{\mathbf{u}\sim c\mathbb{D}_L}|(\partial/\partial w)\Gamma_{\text{S6}}(\mathbf{u})_L|}{\mathbb{E}_{\mathbf{u}\sim c\mathbb{D}_L}|(\partial/\partial b)\Gamma_{\text{S4D}}(\mathbf{u})_L|} = \Omega(c^3), \qquad \frac{\mathbb{E}_{\mathbf{u}\sim c\mathbb{D}_L}|(\partial/\partial b)\Gamma_{\text{S6}}(\mathbf{u})_L|}{\mathbb{E}_{\mathbf{u}\sim c\mathbb{D}_L}|(\partial/\partial b)\Gamma_{\text{S4D}}(\mathbf{u})_L|} = \Omega(c^2), \qquad c \to \infty.$$
2. An S6 model is less stable to train than an S4D model as the input length increases. That is, fix $w = 0$. There exists a sequence $b(L) \to -\infty$ as $L \to \infty$, such that given any sequence of distributions $\mathbb{D}_L$ on $[0,1]^{L-1} \times \{1\}$ with $\mathbb{E}_{\mathbf{u}\sim\mathbb{D}_L}[\Gamma_{\text{S4D}}(\mathbf{u})_L] = 0$, $c_1 \leq \text{Var}_{\mathbf{u}\sim\mathbb{D}_L}[u_j] \leq c_2$ for all $1 \leq j \leq L-1$, where $c_1, c_2 > 0$ are universal constants, and $\left|\sum_{1\leq i<j\leq L} \text{Cov}(\overline{\mathbf{A}}^{L-i}u_i, \overline{\mathbf{A}}^{L-j}u_j)\right| = \mathcal{O}(L)$, where $\overline{\mathbf{A}} = \exp(\exp(b(L))\mathbf{A})$, we have for a.e. $\mathbf{C} \in \mathbb{R}^{1\times n}$ that
$$\limsup_{L\to\infty} \left(\frac{\mathbb{E}_{\mathbf{u}\sim\mathbb{D}_L}|(\partial/\partial b(L))\Gamma_{\text{S6}}(\mathbf{u})_L|}{\mathbb{E}_{\mathbf{u}\sim\mathbb{D}_L}|(\partial/\partial b(L))\Gamma_{\text{S4D}}(\mathbf{u})_L|}\right) \Big/ \sqrt{L} > 0.$$

The first part of our result shows that an S6 model becomes increasingly unstable relative to an S4D model as the input size grows. This is expected, as the matrices $\overline{\mathbf{B}}_k^{(i)}$ and $\overline{\mathbf{C}}_k$ in eq. (3) depend linearly on the input $\mathbf{u}_k$. However, this effect is typically mitigated in practice by input normalization and is therefore of less practical concern. The more significant insight lies in the second part of the theorem: as the sequence length L increases, the S6 model also becomes less stable to train. This is particularly relevant in the context of LRA tasks, where sequences can be extremely long; for example, the `PathX` task involves sequences of length 16384. In such cases, the training stability of S6 and S4D are dramatically different. Note that we have made some technical assumptions. First, to preserve long-range dependencies as $L \to \infty$, the sampling interval Δ must shrink. This justifies why we assumed $b(L) \to -\infty$ so that $\Delta \to 0^+$ as $L \to \infty$. Second, since the pairwise covariances between $\overline{\mathbf{A}}^{L-i}u_i$ and $\overline{\mathbf{A}}^{L-j}u_j$ can be both positive and negative, cancellation occurs and assuming their total sum scales as $\mathcal{O}(L)$ is mild and reflects the natural behavior of aggregated dependencies in long sequences. We also fixed $w = 0$, leaving the case when $w \neq 0$ for future work. More numerical and empirical experiments that illustrate Theorem 3 can be found in Appendix E.

6 B_2S_6: an expressive, gently biased, and stable selective model

We introduce B_2S_6 (Block-Biased-S6) to address the shortcomings of S6. Given an input sequence $\mathbf{u} = (\mathbf{u}_1, \ldots, \mathbf{u}_L)$, where $\mathbf{u}_k \in \mathbb{R}^{d\times 1}$ for $1 \leq k \leq L$, we assume that $d = h \times p$ for two hyperparameters $h, p \geq 1$. We then partition each input vector into h sub-vectors of size p: $\mathbf{u}_k = \begin{bmatrix}{}^1\mathbf{u}_k^\top & \cdots & {}^h\mathbf{u}_k^\top\end{bmatrix}^\top$. Note that we use a left-superscript for the block index. Then, the output of a B_2S_6 unit is a sequence $\Gamma_{\text{B}_2\text{S}_6}(\mathbf{u}) = \mathbf{y} = (\mathbf{y}_1, \ldots, \mathbf{y}_L)$, where each output vector can also be partitioned into h sub-vectors of size p, i.e., $\mathbf{y}_k = \begin{bmatrix}{}^1\mathbf{y}_k^\top & \cdots & {}^h\mathbf{y}_k^\top\end{bmatrix}^\top$, defined by
$${}^j\mathbf{x}_k^{(i)} = {}^j\overline{\mathbf{A}}_k^{(i)}\,{}^j\mathbf{x}_{k-1}^{(i)} + {}^j\overline{\mathbf{B}}_k^{(i)}\,{}^j\mathbf{u}_k^{(i)}, \quad {}^j\mathbf{y}_k^{(i)} = {}^j\overline{\mathbf{C}}_k\,{}^j\mathbf{x}_k^{(i)}, \qquad 1 \leq i \leq p, \qquad 1 \leq j \leq h, \quad (7)$$

where ${}^j\mathbf{x}_k^{(i)} \in \mathbb{R}^n$, ${}^j\mathbf{u}_k^{(i)} \in \mathbb{R}$, ${}^j\mathbf{y}_k^{(i)} \in \mathbb{R}$, and the matrices ${}^j\overline{\mathbf{A}}_k^{(i)} \in \mathbb{R}^{n\times n}$, ${}^j\overline{\mathbf{B}}_k^{(i)} \in \mathbb{R}^{n\times 1}$, and ${}^j\overline{\mathbf{C}}_k \in \mathbb{R}^{1\times n}$ are input-dependent and computed at each step k as

$$\begin{aligned} {}^j\overline{\mathbf{A}}_k^{(i)} &= \exp({}^j\Delta_k^{(i)}\mathbf{A}), \quad {}^j\Delta_k^{(i)} = \text{softplus}({}^j\mathbf{w}^\top\, {}^j\mathbf{u}_k + {}^jb^{(i)}), \\ {}^j\overline{\mathbf{B}}_k^{(i)} &= \mathbf{A}^{-1}({}^j\overline{\mathbf{A}}_k^{(i)} - \mathbf{I})({}^j\mathbf{B}_{\text{weight}}\, {}^j\mathbf{u}_k + {}^j\mathbf{B}_{\text{bias}}^{(i)}), \quad \overline{\mathbf{C}}_k = {}^j\mathbf{u}_k^\top\, {}^j\mathbf{C}, \end{aligned} \qquad 1 \le k \le L. \tag{8}$$

The trainable parameters are $\mathbf{A} \in \mathbb{R}^{n\times n}$, ${}^j\mathbf{B}_{\text{weight}} \in \mathbb{R}^{n\times p}$, ${}^j\mathbf{B}_{\text{bias}}^{(i)} \in \mathbb{R}^{n\times 1}$, ${}^j\mathbf{C} \in \mathbb{R}^{p\times n}$, ${}^j\mathbf{w} \in \mathbb{R}^{p\times 1}$, and ${}^jb^{(i)} \in \mathbb{R}$, for every $1 \le i \le p$ and $1 \le j \le h$. The pseudocode for B_2S_6 is given in Algorithm 2, which compares to Algorithm 1 for S6 found in the Mamba paper [25], where $s_\Delta(\cdot) = \text{Broadcast}_d(\text{Linear}_1(\cdot))$ and ${}^js_\Delta(\cdot) = \text{Broadcast}_p(\text{Linear}_1(\cdot))$ for every $1 \le j \le h$.

Algorithm 1 S6 Forward Pass

Input: $\mathbf{x} : (B\ L\ d)$
Output: $\mathbf{y} : (B\ L\ d)$

$\mathbf{B}_{\text{S6}} : (B\ L\ n), \quad \mathbf{B}_{\text{S6}}(i,j,:) \leftarrow \mathbf{B}\mathbf{x}(i,j,:)$
$\mathbf{C}_{\text{S6}} : (B\ L\ n), \quad \mathbf{C}_{\text{S6}}(i,j,:) \leftarrow \mathbf{x}(i,j,:)^\top\mathbf{C}$
$\Delta : (B\ L\ d) \leftarrow \text{softplus}(s_\Delta(\mathbf{x}) + \mathbf{b})$
$\overline{\mathbf{A}}, \overline{\mathbf{B}} : (B\ L\ d\ n) \leftarrow \text{discretize}(\Delta, \mathbf{A}, \mathbf{B}_{\text{S6}})$
$\mathbf{y} \leftarrow \text{SSM}(\overline{\mathbf{A}}, \overline{\mathbf{B}}, \mathbf{C}_{\text{S6}})(\mathbf{x})$

Algorithm 2 B_2S_6 Forward Pass

Input: $\mathbf{x} : (B\ L\ d)$
Output: $\mathbf{y} : (B\ L\ d)$

parfor $j = 1 : h$ **do** ▷ independent for every block
  ${}^jI \leftarrow (jp - p + 1) : jp$ ▷ block index
  ${}^j\mathbf{B} : (B\ L\ n), \quad {}^j\mathbf{B}(i,j,:) \leftarrow {}^j\mathbf{B}_{\text{weight}}\mathbf{x}(i,j,{}^jI)$
  ${}^j\mathbf{B} : (B\ L\ p\ n) \leftarrow \text{Broadcast}_p({}^j\mathbf{B}) + \text{Broadcast}_L({}^j\mathbf{B}_{\text{bias}})$
  ${}^j\mathbf{C} : (B\ L\ n), \quad {}^j\mathbf{C}(i,j,:) \leftarrow \mathbf{x}(i,j,{}^jI)^\top {}^j\mathbf{C}$
  ${}^j\Delta : (B\ L\ p) \leftarrow \text{softplus}({}^js_\Delta(\mathbf{x}(:,:,{}^jI)) + {}^j\mathbf{b})$
  ${}^j\overline{\mathbf{A}}, {}^j\overline{\mathbf{B}} : (B\ L\ p\ n) \leftarrow \text{discretize}({}^j\Delta, \mathbf{A}, {}^j\mathbf{B})$
  $\mathbf{y}(:,:,{}^jI) \leftarrow \text{SSM}({}^j\overline{\mathbf{A}}, {}^j\overline{\mathbf{B}}, {}^j\mathbf{C})(\mathbf{x}(:,:,{}^jI))$
end parfor

Comparing the B_2S_6 unit in eq. (7) to the S6 unit in eq. (3), we highlight two key differences (see Figure 1). First, B_2S_6 partitions the d-dimensional input into h blocks of p-dimensional sub-vectors and applies an independent recurrent unit to each block. Second, we introduce a bias term ${}^j\mathbf{B}_{\text{bias}}^{(i)}$ in the computation of the input matrix ${}^j\overline{\mathbf{B}}_k$. While this term is input-independent, it varies across channels, increasing the model's effective width. We do not claim that we invented the block unit design, which was previously suggested in the Mamba2 paper [20], but in this work, we rigorously demonstrate how the combination of block structure and channel-specific bias enhances the expressiveness and generalization of the model on long-range sequence modeling tasks.

First, we show that unlike an S6 model, a B_2S_6 model regains the universal approximation property studied in Theorem 1 by introducing *either* the block unit *or* the bias unit.

Theorem 4. Fix a constant for ${}^j\Delta_k^{(i)}$ for all i, j, and k in eq. (7). The following two statements hold:

1. The block unit alone makes B_2S_6 a universal approximator. More precisely, set ${}^j\mathbf{B}_{\text{bias}}^{(i)} = \mathbf{0}$ for all i and j, and let $\sigma : \mathbb{R} \to \mathbb{R}$ be any Lipschitz continuous, non-polynomial activation function. Given any continuous function $G : [0,1]^{L-1} \times \{1\} \to \mathbb{R}$ and any $\epsilon > 0$. There exist some h and p with $h \times p = d \ge 1$, $n \ge 1$, and a choice of parameters $\mathbf{M}, \mathbf{N}, \boldsymbol{\theta}, \mathbf{A}, {}^j\mathbf{B}_{\text{weight}}$, and ${}^j\mathbf{C}$, where $1 \le j \le h$, such that the map $\tilde{G}$ in eq. (5) with $\Gamma = \Gamma_{\text{B}_2\text{S}_6}$ in eq. (7) satisfies that
$$|\tilde{G}(\mathbf{u}) - G(\mathbf{u})| \le \epsilon, \qquad \text{for any } \mathbf{u} \in [0,1]^{L-1} \times \{1\}.$$
2. The bias unit alone makes B_2S_6 a universal approximator. More precisely, set $h = 1$ and $p = d$, and let $\sigma : \mathbb{R} \to \mathbb{R}$ be any Lipschitz continuous, non-polynomial activation function. Given any continuous function $G : [0,1]^{L-1} \times \{1\} \to \mathbb{R}$ and any $\epsilon > 0$. There exist some $d \ge 1$, $n \ge 1$, and a choice of parameters $\mathbf{M}, \mathbf{N}, \boldsymbol{\theta}, \mathbf{A}, {}^1\mathbf{B}_{\text{weight}}$, ${}^1\mathbf{B}_{\text{bias}}^{(i)}$, and ${}^1\mathbf{C}$, where $1 \le i \le d$, such that the map $\tilde{G}$ in eq. (5) with $\Gamma = \Gamma_{\text{B}_2\text{S}_6}$ in eq. (7) satisfies that
$$|\tilde{G}(\mathbf{u}) - G(\mathbf{u})| \le \epsilon, \qquad \text{for any } \mathbf{u} \in [0,1]^{L-1} \times \{1\}.$$

The block design and channel-specific bias in the B_2S_6 model significantly enhance its expressiveness, enabling it to handle more complex sequential tasks that benefit from wider neural networks. To illustrate this, we revisit the experiment from section 3, this time using only the block structure

(without the bias term), noting that the addition of the bias would only further improve performance. As shown in Figure 2, unlike an S6 model, the performance of the $\mathrm{B_2S_6}$ model improves substantially as d increases, holding the ratio h/p constant.

In contrast to the S6 model, the $\mathrm{B_2S_6}$ architecture introduces a gentler inductive bias that is better suited for long-range tasks. Instead of Theorem 2, we now establish the following result.

Theorem 5. Fix a $k_0 < L$ and let $\mathbf{A} \in \mathbb{R}^{n\times n}$ be a diagonal matrix with negative diagonal entries. For a.e. input sequence $\mathbf{u} = (\mathbf{u}_1, \dots, \mathbf{u}_L) \in \mathbb{R}^L$ such that there exist j_1 and j_2 with ${}^{j_1}\mathbf{w}^\top\, {}^{j_1}\mathbf{u}_{k_0} > 0$ and ${}^{j_2}\mathbf{w}^\top\, {}^{j_2}\mathbf{u}_{k_0} < 0$, and a.e. parameters ${}^{j}\mathbf{B}_{\text{weight}}$, ${}^{j}\mathbf{B}_{\text{bias}}^{(i)}$, ${}^{j}\mathbf{C}$, and ${}^{j}b^{(i)}$, where $1 \le j \le h$ and $1 \le i \le p$, let $S_{\mathrm{B_2S_6},k}$ be defined in eq. (6), where $\Gamma = \Gamma_{\mathrm{B_2S_6}}$ is defined in eq. (7). We have

$$S_{\mathrm{B_2S_6},k}((\mathbf{u}_1, \dots, \mathbf{u}_{k_0-1}, c\mathbf{u}_{k_0}, \mathbf{u}_{k_0+1}, \dots, \mathbf{u}_L)) = \begin{cases} \mathcal{O}(|c|^{-2}) & , k < k_0, \\ \mathcal{O}(|c|^{-1}) & , k = k_0, \\ \Theta(1) & , k > k_0, \end{cases} \qquad c \to \pm\infty.$$

If each ${}^{j}\mathbf{w}$ is randomly initialized for $1 \le j \le h$, then the probabilities that a given input satisfies ${}^{j}\mathbf{w}^\top\, {}^{j}\mathbf{u}_{k_0} < 0$ and ${}^{j}\mathbf{w}^\top\, {}^{j}\mathbf{u}_{k_0} > 0$ are equal. As a result, the probability that the assumptions in Theorem 5 are violated vanishes exponentially with the number of blocks h. Compared to Theorem 2, this means that $\mathrm{B_2S_6}$ exhibits a significantly milder inductive bias in the presence of large inputs, avoiding exponentially decaying effects as the input magnitude increases. This behavior is confirmed by the experiment in section 4, where $\mathrm{B_2S_6}$ maintains strong performance even when σ_1 is very small and σ_2 is very large. Lastly, while the block and bias components improve expressiveness and inductive bias, they do not directly resolve the training instability that arises with long sequences. Therefore, for LRA tasks, we reduce the learning rates of ${}^{j}\mathbf{w}$ and ${}^{j}b^{(i)}$ to improve training stability.[3]

7 Experiments

Ablation. In this paper, we show that the $\mathrm{B_2S_6}$ model achieves strong performance on the LRA benchmark. Compared to the standard Mamba model, our $\mathrm{B_2S_6}$ variant incorporates a multihead structure and a bias term $\mathbf{B}_{\text{bias}}$, and uses complex-valued parameters for $\mathrm{diag}(\mathbf{A})$, $\mathbf{B}_{\text{weight}}$, and $\mathbf{B}_{\text{bias}}$ (see [64, 97, 47]). Before presenting full LRA results, we demonstrate the utility of each modification in Table 2. The second column shows model accuracy without bias terms, the third without complex parameterization, and all rows below the first use the multihead structure. As seen in Table 2, all three components contribute positively to the performance on the sCIFAR-10 task. An interesting observation is that, when $d = h \times p$ is fixed, model accuracy increases monotonically with h only in the absence of $\mathbf{B}_{\text{bias}}$. This should not be surprising: if $\mathbf{B}_{\text{bias}} = \mathbf{0}$, the model's effective width is h, so larger h improves expressiveness and generalization. However, once $\mathbf{B}_{\text{bias}}$ is introduced, the model already attains high effective (though non-selective) width even when $h = 1$ because ${}^{j}\mathbf{B}_{\text{bias}}^{(i)}$ varies with i. Thus, increasing h trades off between more selective blocks, which improves the *quantity* of selectivity, and reduced receptive field ${}^{j}\mathbf{u}_k$ per block, which impairs the *quality* of each selection.

Long-Range Arena. In Table 3, we see that our $\mathrm{B_2S_6}$ model outperforms many selective and non-selective models on LRA. In particular, it is the first selective SSM we are aware of that achieves state-of-the-art performance on this benchmark. A more comprehensive table is found in Appendix F.

Language Tasks. While our primary goal is not to train a large language model (LLM), we conduct a preliminary evaluation of $\mathrm{B_2S_6}$'s language modeling capability using a sampled version of the SlimPajama-627B dataset [78]. For each model family, we train a model with approximately 30 layers, corresponding to approximately 250M parameters. The precise number of layers varies slightly with models to make the number of parameters roughly the same. We train four models for one epoch and report the perplexity statistics. We only vary the recurrent unit without changing the rest of the model architecture. That is, all models are based on the Mamba architecture proposed in [25, Fig. 3]:

$$\mathbf{y} = \Gamma(\sigma(\mathrm{Conv}(\mathrm{Linear}(\mathbf{x})))) \circ \sigma(\mathrm{Linear}(\mathbf{x})),$$

[3] In general, freezing some of the other parameters indeed helps stabilize the training, but it also puts us at risk of converging to bad minima. For example, we observed that it never works to freeze $\mathbf{B}$ and $\mathbf{C}$, and that freezing the matrix $\mathbf{A}$ and $\mathbf{D}$ usually does not have a big impact, given that they are initialized properly (see [26, 97]).

Table 2: Ablation study of our B_2S_6 model. We train a model to learn the sCIFAR-10 task, where we fix $d = 128$ and change the number of blocks h and the size of each block p (see eq. (7)). For each pair of h and p, we train a full B_2S_6 model with complex parameters, a B_2S_6 model with complex parameters but no bias term, and a full B_2S_6 model with real parameters. A more greenish color indicates a better accuracy, while a more reddish color labels a worse accuracy.

		With B_{bias} (Complex)	Without B_{bias} (Complex)	With B_{bias} (Real)
h	p	Accuracy ± Std	Accuracy ± Std	Accuracy ± Std
1	128	**81.56** ± 1.22	**71.77** ± 1.88	**47.82** ± 5.42
2	64	**84.83** ± 0.73	**79.44** ± 1.10	**54.40** ± 0.35
4	32	**83.86** ± 1.38	**80.93** ± 0.94	**54.77** ± 0.54
8	16	**87.19** ± 0.26	**81.54** ± 1.14	**53.81** ± 0.87
16	8	**87.04** ± 0.33	**83.78** ± 0.79	**51.79** ± 3.61
32	4	**85.83** ± 0.80	**84.11** ± 0.39	**56.18** ± 0.18
64	2	**86.30** ± 0.60	**84.27** ± 0.76	**52.03** ± 2.04
128	1	**85.32** ± 0.55	**84.79** ± 0.43	**56.45** ± 0.71

Table 3: Test accuracies in the Long-Range Arena of different variants of SSMs. A bold number indicates the best accuracy on a task while an underlined number corresponds to the second best.

Model	ListOps	Text	Retrieval	Image	Pathfinder	Path-X	Avg.
S4 [28]	59.60	86.82	90.90	<u>88.65</u>	94.20	96.35	86.09
S4D [27]	60.47	86.18	89.46	88.19	93.06	91.95	84.89
S5 [77]	62.15	**89.31**	91.40	88.00	<u>95.33</u>	**98.58**	<u>87.46</u>
S6 (Mamba) [25]	38.02	82.98	72.14	69.82	69.26	67.32	66.59
S7 [79]	<u>63.77</u>	87.22	**91.80**	61.14	65.62	61.50	71.82
Mamba2 [20]	41.45	86.09	79.23	71.96	75.45	69.07	70.54
B_2S_6 (ours)	**63.85** ±0.45	<u>88.32</u> ±0.50	<u>91.44</u> ±0.36	**88.81** ±0.22	**95.93** ±0.38	<u>97.90</u> ±0.17	**87.71**

where $\circ$ stands for the Hadamard product and we only change Γ in three models to be $\Gamma_{S4D}, \Gamma_{S6}$, Γ_{Mamba2}, and $\Gamma_{B_2S_6}$, respectively. We find that introducing the bias term $\mathbf{B}_{bias}$ only makes the training of a B_2S_6 model 2.7% slower than an S6 model of comparable size. Yet, the perplexity of B_2S_6 closely matches that of S6, showing the versatility of our model.

Figure 4: Perplexity over training steps for an S6, Mamba2, B_2S_6, and S4D model. The dataset is SlimPajama-6B, a sampled version of the SlimPajama-627B dataset.

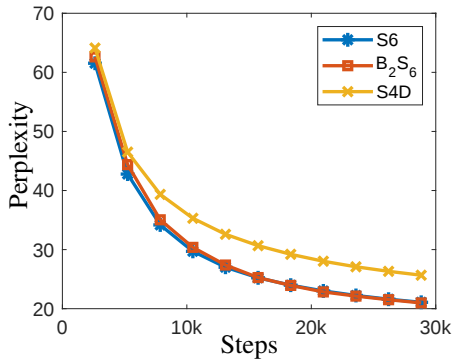

Steps	S6	Mamba2	B_2S_6	S4D
2620	61.5441	59.6233	62.6133	64.1203
5241	42.7838	39.8305	44.3846	46.5118
7862	34.1740	31.9994	35.0440	39.3496
10483	29.7074	27.0987	30.3787	35.3028
13104	27.0171	25.2930	27.3891	32.5946
15725	25.2265	24.0179	25.2668	30.6639
18346	23.9789	23.1224	23.9370	29.2052
20967	23.0044	22.3695	22.8394	28.0314
23588	22.2368	21.7509	22.1322	27.0897
26209	21.6068	21.2480	21.5206	26.3221
28830	21.0785	20.8218	20.9773	25.6661

8 Conclusion

In this work, we provided a theoretical analysis of Mamba's limitations in modeling long-range sequences, focusing on expressiveness, inductive bias, and training stability. We proposed a new model, B_2S_6, which introduces a block structure and channel-specific bias to improve upon each of these dimensions. Empirical results demonstrate that B_2S_6 significantly enhances performance on long-range sequence tasks while maintaining versatility across domains. Future work includes a more detailed analysis of training stability across all Mamba parameters, exploring architectural refinements to further mitigate instability, studying the training dynamics of Mamba and B_2S_6 to better characterize their inductive biases, and scaling up B_2S_6 as a language or foundation model.

Acknowledgments

AY was partially supported by the Office of Naval Research under Grant Number N00014-23-1-2729 and NSF DMS-2319621. NBE would like to acknowledge the U.S. Department of Energy, under Contract Number DE-AC02-05CH11231 and DE-AC02-05CH11231, for providing partial support of this work.

References

[1] Naman Agarwal, Daniel Suo, Xinyi Chen, and Elad Hazan. Spectral state space models. *arXiv preprint arXiv:2312.06837*, 2023.

[2] Zeyuan Allen-Zhu, Yuanzhi Li, and Yingyu Liang. Learning and generalization in overparameterized neural networks, going beyond two layers. *Advances in neural information processing systems*, 32, 2019.

[3] Carmen Amo Alonso, Jerome Sieber, and Melanie N Zeilinger. State space models as foundation models: A control theoretic overview. *arXiv preprint arXiv:2403.16899*, 2024.

[4] Marco Ancona, Enea Ceolini, Cengiz Öztireli, and Markus Gross. Towards better understanding of gradient-based attribution methods for deep neural networks. *arXiv preprint arXiv:1711.06104*, 2017.

[5] Alessio Ansuini, Alessandro Laio, Jakob H Macke, and Davide Zoccolan. Intrinsic dimension of data representations in deep neural networks. *Advances in Neural Information Processing Systems*, 32, 2019.

[6] Martin Arjovsky, Amar Shah, and Yoshua Bengio. Unitary evolution recurrent neural networks. In *International Conference on Machine Learning*, pages 1120–1128. PMLR, 2016.

[7] Sanjeev Arora, Simon Du, Wei Hu, Zhiyuan Li, and Ruosong Wang. Fine-grained analysis of optimization and generalization for overparameterized two-layer neural networks. In *International conference on machine learning*, pages 322–332. PMLR, 2019.

[8] David Baehrens, Timon Schroeter, Stefan Harmeling, Motoaki Kawanabe, Katja Hansen, and Klaus-Robert Müller. How to explain individual classification decisions. *The Journal of Machine Learning Research*, 11:1803–1831, 2010.

[9] Shaojie Bai, J Zico Kolter, and Vladlen Koltun. An empirical evaluation of generic convolutional and recurrent networks for sequence modeling. *arXiv preprint arXiv:1803.01271*, 2018.

[10] Peter L Bartlett, Andrea Montanari, and Alexander Rakhlin. Deep learning: a statistical viewpoint. *Acta numerica*, 30:87–201, 2021.

[11] Ronen Basri, David Jacobs, Yoni Kasten, and Shira Kritchman. The convergence rate of neural networks for learned functions of different frequencies. *Adv. Neur. Info. Proc. Syst.*, 32, 2019.

[12] Gregory Beylkin. Fast convolution algorithm for state space models. *arXiv preprint arXiv:2411.17729*, 2024.

[13] Bo Chang, Minmin Chen, Eldad Haber, and Ed H Chi. Antisymmetricrnn: A dynamical system view on recurrent neural networks. In *International Conference on Machine Learning*, 2019.

[14] Pratik Chaudhari, Anna Choromanska, Stefano Soatto, Yann LeCun, Carlo Baldassi, Christian Borgs, Jennifer Chayes, Levent Sagun, and Riccardo Zecchina. Entropy-sgd: Biasing gradient descent into wide valleys. *Journal of Statistical Mechanics: Theory and Experiment*, 2019(12):124018, 2019.

[15] Tianping Chen and Hong Chen. Universal approximation to nonlinear operators by neural networks with arbitrary activation functions and its application to dynamical systems. *IEEE Transactions on Neural Networks*, 6(4):911–917, 1995.

[16] Anna Choromanska, Mikael Henaff, Michael Mathieu, Gérard Ben Arous, and Yann LeCun. The loss surfaces of multilayer networks. In *Artificial intelligence and statistics*, pages 192–204. PMLR, 2015.

[17] Krzysztof Choromanski, Valerii Likhosherstov, David Dohan, Xingyou Song, Andreea Gane, Tamas Sarlos, Peter Hawkins, Jared Davis, Afroz Mohiuddin, Lukasz Kaiser, et al. Rethinking attention with performers. In *International Conference on Machine Learning*, 2020.

[18] George Cybenko. Approximation by superpositions of a sigmoidal function. *Mathematics of control, signals and systems*, 2(4):303–314, 1989.

[19] Alex Damian, Eshaan Nichani, and Jason D Lee. Self-stabilization: The implicit bias of gradient descent at the edge of stability. *International Conference on Learning Representations*, 2023.

[20] Tri Dao and Albert Gu. Transformers are ssms: Generalized models and efficient algorithms through structured state space duality. *arXiv preprint arXiv:2405.21060*, 2024.

[21] Yann N Dauphin, Razvan Pascanu, Caglar Gulcehre, Kyunghyun Cho, Surya Ganguli, and Yoshua Bengio. Identifying and attacking the saddle point problem in high-dimensional non-convex optimization. *Advances in neural information processing systems*, 27, 2014.

[22] N Benjamin Erichson, Omri Azencot, Alejandro Queiruga, Liam Hodgkinson, and Michael W Mahoney. Lipschitz recurrent neural networks. In *International Conference on Learning Representations*, 2021.

[23] Xavier Glorot and Yoshua Bengio. Understanding the difficulty of training deep feedforward neural networks. In *Proceedings of the thirteenth international conference on artificial intelligence and statistics*, pages 249–256. JMLR Workshop and Conference Proceedings, 2010.

[24] Riccardo Grazzi, Julien Siems, Arber Zela, Jörg KH Franke, Frank Hutter, and Massimiliano Pontil. Unlocking state-tracking in linear rnns through negative eigenvalues. *International Conference on Learning Representations*, 2025.

[25] Albert Gu and Tri Dao. Mamba: Linear-time sequence modeling with selective state spaces. *arXiv preprint arXiv:2312.00752*, 2023.

[26] Albert Gu, Tri Dao, Stefano Ermon, Atri Rudra, and Christopher Ré. Hippo: Recurrent memory with optimal polynomial projections. *Advances in neural information processing systems*, 33:1474–1487, 2020.

[27] Albert Gu, Karan Goel, Ankit Gupta, and Christopher Ré. On the parameterization and initialization of diagonal state space models. *Advances in Neural Information Processing Systems*, 35:35971–35983, 2022.

[28] Albert Gu, Karan Goel, and Christopher Re. Efficiently modeling long sequences with structured state spaces. In *International Conference on Learning Representations*, 2022.

[29] Ankit Gupta, Albert Gu, and Jonathan Berant. Diagonal state spaces are as effective as structured state spaces. *Advances in Neural Information Processing Systems*, 35:22982–22994, 2022.

[30] Ramin Hasani, Mathias Lechner, Tsun-Hsuan Wang, Makram Chahine, Alexander Amini, and Daniela Rus. Liquid structural state-space models. *International Conference on Learning Representations*, 2023.

[31] Kaiming He, Xiangyu Zhang, Shaoqing Ren, and Jian Sun. Deep residual learning for image recognition. In *Proceedings of the IEEE conference on computer vision and pattern recognition*, pages 770–778, 2016.

[32] Arya Honarpisheh, Mustafa Bozdag, Mario Sznaier, and Octavia Camps. Generalization error analysis for selective state-space models through the lens of attention. *arXiv preprint arXiv:2502.01473*, 2025.

[33] Zheyuan Hu, Nazanin Ahmadi Daryakenari, Qianli Shen, Kenji Kawaguchi, and George Em Karniadakis. State-space models are accurate and efficient neural operators for dynamical systems. *arXiv preprint arXiv:2409.03231*, 2024.

[34] Sukjun Hwang, Aakash Sunil Lahoti, Ratish Puduppully, Tri Dao, and Albert Gu. Hydra: Bidirectional state space models through generalized matrix mixers. *Advances in Neural Information Processing Systems*, 37:110876–110908, 2024.

[35] A. Jacot, F. Gabriel, and C. Hongler. Neural tangent kernel: Convergence and generalization in neural networks. *Adv. Neur. Info. Proc. Syst.*, 31, 2018.

[36] Rudolph Emil Kalman. A new approach to linear filtering and prediction problems. *J. Basic Eng*, 82(1):35–45, 1960.

[37] Angelos Katharopoulos, Apoorv Vyas, Nikolaos Pappas, and François Fleuret. Transformers are rnns: Fast autoregressive transformers with linear attention. In *International conference on machine learning*, pages 5156–5165. PMLR, 2020.

[38] Nitish Shirish Keskar, Dheevatsa Mudigere, Jorge Nocedal, Mikhail Smelyanskiy, and Ping Tak Peter Tang. On large-batch training for deep learning: Generalization gap and sharp minima. *International Conference on Learning Representations*, 2017.

[39] Patrick Kidger and Terry J. Lyons. Universal approximation with deep narrow networks. *CoRR*, abs/1905.08539, 2019.

[40] Sungyoon Kim, Aaron Mishkin, and Mert Pilanci. Exploring the loss landscape of regularized neural networks via convex duality. *International Conference on Learning Representations*, 2025.

[41] Nikita Kitaev, Łukasz Kaiser, and Anselm Levskaya. Reformer: The efficient transformer. In *International Conference on Machine Learning*, 2020.

[42] Hao Li, Zheng Xu, Gavin Taylor, Christoph Studer, and Tom Goldstein. Visualizing the loss landscape of neural nets. *Advances in neural information processing systems*, 31, 2018.

[43] Kai Li, Guo Chen, Runxuan Yang, and Xiaolin Hu. Spmamba: State-space model is all you need in speech separation. *arXiv preprint arXiv:2404.02063*, 2024.

[44] Kunchang Li, Xinhao Li, Yi Wang, Yinan He, Yali Wang, Limin Wang, and Yu Qiao. Videomamba: State space model for efficient video understanding. In *European Conference on Computer Vision*, pages 237–255. Springer, 2024.

[45] Opher Lieber, Barak Lenz, Hofit Bata, Gal Cohen, Jhonathan Osin, Itay Dalmedigos, Erez Safahi, Shaked Meirom, Yonatan Belinkov, Shai Shalev-Shwartz, et al. Jamba: A hybrid transformer-mamba language model. *International Conference on Learning Representations*, 2025.

[46] Fusheng Liu and Qianxiao Li. From generalization analysis to optimization designs for state space models. *arXiv preprint arXiv:2405.02670*, 2024.

[47] Fusheng Liu and Qianxiao Li. Autocorrelation matters: Understanding the role of initialization schemes for state space models. *International Conference on Learning Representations*, 2025.

[48] Ziwei Liu, Qidong Liu, Yejing Wang, Wanyu Wang, Pengyue Jia, Maolin Wang, Zitao Liu, Yi Chang, and Xiangyu Zhao. Sigma: Selective gated mamba for sequential recommendation. In *Proceedings of the AAAI Conference on Artificial Intelligence*, volume 39, pages 12264–12272, 2025.

[49] Ilya Loshchilov and Frank Hutter. Sgdr: Stochastic gradient descent with warm restarts. *International Conference on Learning Representations*, 2017.

[50] Lu Lu, Pengzhan Jin, Guofei Pang, Zhongqiang Zhang, and George Em Karniadakis. Learning nonlinear operators via deeponet based on the universal approximation theorem of operators. *Nature machine intelligence*, 3(3):218–229, 2021.

[51] Haoyu Ma, Yushu Chen, Wenlai Zhao, Jinzhe Yang, Yingsheng Ji, Xinghua Xu, Xiaozhu Liu, Hao Jing, Shengzhuo Liu, and Guangwen Yang. A mamba foundation model for time series forecasting. *arXiv preprint arXiv:2411.02941*, 2024.

[52] Song Mei, Andrea Montanari, and Phan-Minh Nguyen. A mean field view of the landscape of two-layer neural networks. *Proceedings of the National Academy of Sciences*, 115(33):E7665–E7671, 2018.

[53] Nicola Muca Cirone, Antonio Orvieto, Benjamin Walker, Cristopher Salvi, and Terry Lyons. Theoretical foundations of deep selective state-space models. *Advances in Neural Information Processing Systems*, 37:127226–127272, 2024.

[54] Yuqi Nie, Nam H Nguyen, Phanwadee Sinthong, and Jayant Kalagnanam. A time series is worth 64 words: Long-term forecasting with transformers. In *The Eleventh International Conference on Learning Representations*, 2023.

[55] Antonio Orvieto, Samuel L Smith, Albert Gu, Anushan Fernando, Caglar Gulcehre, Razvan Pascanu, and Soham De. Resurrecting recurrent neural networks for long sequences. *arXiv preprint arXiv:2303.06349*, 2023.

[56] Rom N Parnichkun, Stefano Massaroli, Alessandro Moro, Jimmy TH Smith, Ramin Hasani, Mathias Lechner, Qi An, Christopher Ré, Hajime Asama, and Stefano Ermon. State-free inference of state-space models: The transfer function approach. *International Conference on Machine Learning*, 2024.

[57] Razvan Pascanu, Tomas Mikolov, and Yoshua Bengio. On the difficulty of training recurrent neural networks. In *International conference on machine learning*, pages 1310–1318. Pmlr, 2013.

[58] Badri Narayana Patro and Vijay Srinivas Agneeswaran. Mamba-360: Survey of state space models as transformer alternative for long sequence modelling: Methods, applications, and challenges. *arXiv preprint arXiv:2404.16112*, 2024.

[59] Yan Ru Pei. Let SSMs be ConvNets: State-space modeling with optimal tensor contractions. *International Conference on Learning Representations*, 2025.

[60] Allan Pinkus. Approximation theory of the mlp model in neural networks. *Acta numerica*, 8:143–195, 1999.

[61] Biqing Qi, Junqi Gao, Dong Li, Kaiyan Zhang, Jianxing Liu, Ligang Wu, and Bowen Zhou. S4++: Elevating long sequence modeling with state memory reply. 2024.

[62] Yanyuan Qiao, Zheng Yu, Longteng Guo, Sihan Chen, Zijia Zhao, Mingzhen Sun, Qi Wu, and Jing Liu. Vl-mamba: Exploring state space models for multimodal learning. *arXiv preprint arXiv:2403.13600*, 2024.

[63] Gokul Raju Govinda Raju, Nikola Zubić, Marco Cannici, and Davide Scaramuzza. Perturbed state space feature encoders for optical flow with event cameras. *arXiv preprint arXiv:2504.10669*, 2025.

[64] Yuval Ran-Milo, Eden Lumbroso, Edo Cohen-Karlik, Raja Giryes, Amir Globerson, and Nadav Cohen. Provable benefits of complex parameterizations for structured state space models. *Advances in Neural Information Processing Systems*, 37:115906–115939, 2024.

[65] Stefano Rando, Luca Romani, Matteo Migliarini, Luca Franco, Denis Gudovskiy, and Fabio Galasso. Serpent: Selective resampling for expressive state space models. *arXiv preprint arXiv:2501.11729*, 2025.

[66] David W Romero, Anna Kuzina, Erik J Bekkers, Jakub M Tomczak, and Mark Hoogendoorn. Ckconv: Continuous kernel convolution for sequential data. In *International Conference on Machine Learning*, 2022.

[67] Grant Rotskoff and Eric Vanden-Eijnden. Trainability and accuracy of artificial neural networks: An interacting particle system approach. *Communications on Pure and Applied Mathematics*, 75(9):1889–1935, 2022.

[68] T Konstantin Rusch and Siddhartha Mishra. Unicornn: A recurrent model for learning very long time dependencies. In *International Conference on Machine Learning*, pages 9168–9178. PMLR, 2021.

[69] T Konstantin Rusch and Daniela Rus. Oscillatory state-space models. *International Conference on Learning Representations*, 2025.

[70] Levent Sagun, Utku Evci, V Ugur Guney, Yann Dauphin, and Leon Bottou. Empirical analysis of the hessian of over-parametrized neural networks. *arXiv preprint arXiv:1706.04454*, 2017.

[71] Anton Maximilian Schäfer and Hans Georg Zimmermann. Recurrent neural networks are universal approximators. In *Artificial Neural Networks–ICANN 2006: 16th International Conference, Athens, Greece, September 10-14, 2006. Proceedings, Part I 16*, pages 632–640. Springer, 2006.

[72] Shuaijie Shen, Chao Wang, Renzhuo Huang, Yan Zhong, Qinghai Guo, Zhichao Lu, Jianguo Zhang, and Luziwei Leng. SpikingSSMs: Learning long sequences with sparse and parallel spiking state space models. In *Proceedings of the AAAI Conference on Artificial Intelligence*, volume 39, pages 20380–20388, 2025.

[73] Avanti Shrikumar, Peyton Greenside, and Anshul Kundaje. Learning important features through propagating activation differences. In *International conference on machine learning*, pages 3145–3153. PMlR, 2017.

[74] Jerome Sieber, Carmen Amo Alonso, Alexandre Didier, Melanie Zeilinger, and Antonio Orvieto. Understanding the differences in foundation models: Attention, state space models, and recurrent neural networks. *Advances in Neural Information Processing Systems*, 37:134534–134566, 2024.

[75] Karen Simonyan, Andrea Vedaldi, and Andrew Zisserman. Deep inside convolutional networks: Visualising image classification models and saliency maps. *International Conference on Learning Representations*, 2014.

[76] Jakub Smékal, Jimmy TH Smith, Michael Kleinman, Dan Biderman, and Scott W Linderman. Towards a theory of learning dynamics in deep state space models. *arXiv preprint arXiv:2407.07279*, 2024.

[77] Jimmy T.H. Smith, Andrew Warrington, and Scott Linderman. Simplified state space layers for sequence modeling. In *The Eleventh International Conference on Learning Representations*, 2023.

[78] Daria Soboleva, Faisal Al-Khateeb, Robert Myers, Jacob R Steeves, Joel Hestness, and Nolan Dey. SlimPajama: A 627B token cleaned and deduplicated version of RedPajama, 2023.

[79] Taylan Soydan, Nikola Zubić, Nico Messikommer, Siddhartha Mishra, and Davide Scaramuzza. S7: Selective and simplified state space layers for sequence modeling. *arXiv preprint arXiv:2410.03464*, 2024.

[80] Namjoon Suh and Guang Cheng. A survey on statistical theory of deep learning: Approximation, training dynamics, and generative models. *Annual Review of Statistics and Its Application*, 12, 2024.

[81] Mukund Sundararajan, Ankur Taly, and Qiqi Yan. Axiomatic attribution for deep networks. In *International conference on machine learning*, pages 3319–3328. PMLR, 2017.

[82] Matus Telgarsky. Benefits of depth in neural networks. In *Conference on learning theory*, pages 1517–1539. PMLR, 2016.

[83] Ashish Vaswani, Noam Shazeer, Niki Parmar, Jakob Uszkoreit, Llion Jones, Aidan N Gomez, Łukasz Kaiser, and Illia Polosukhin. Attention is all you need. *Advances in neural information processing systems*, 30, 2017.

[84] Roger Waleffe, Wonmin Byeon, Duncan Riach, Brandon Norick, Vijay Korthikanti, Tri Dao, Albert Gu, Ali Hatamizadeh, Sudhakar Singh, Deepak Narayanan, et al. An empirical study of mamba-based language models. *arXiv preprint arXiv:2406.07887*, 2024.

[85] Maolin Wang, Sheng Zhang, Ruocheng Guo, Wanyu Wang, Xuetao Wei, Zitao Liu, Hongzhi Yin, Yi Chang, and Xiangyu Zhao. Star-rec: Making peace with length variance and pattern diversity in sequential recommendation. *arXiv preprint arXiv:2505.03484*, 2025.

[86] Shida Wang and Qianxiao Li. StableSSM: Alleviating the curse of memory in state-space models through stable reparameterization. *arXiv preprint arXiv:2311.14495*, 2023.

[87] Shida Wang and Beichen Xue. State-space models with layer-wise nonlinearity are universal approximators with exponential decaying memory. *Advances in Neural Information Processing Systems*, 36, 2024.

[88] Shida Wang and Beichen Xue. State-space models with layer-wise nonlinearity are universal approximators with exponential decaying memory. *Advances in Neural Information Processing Systems*, 36, 2024.

[89] Xiao Wang, Shiao Wang, Yuhe Ding, Yuehang Li, Wentao Wu, Yao Rong, Weizhe Kong, Ju Huang, Shihao Li, Haoxiang Yang, et al. State space model for new-generation network alternative to transformers: A survey. *arXiv preprint arXiv:2404.09516*, 2024.

[90] Yihan Wang, Lujun Zhang, Annan Yu, N Benjamin Erichson, and Tiantian Yang. A deep state space model for rainfall-runoff simulations. *arXiv preprint arXiv:2501.14980*, 2025.

[91] Zihan Wang, Fanheng Kong, Shi Feng, Ming Wang, Xiaocui Yang, Han Zhao, Daling Wang, and Yifei Zhang. Is mamba effective for time series forecasting? *Neurocomputing*, 619:129178, 2025.

[92] Lechao Xiao, Jeffrey Pennington, and Samuel Schoenholz. Disentangling trainability and generalization in deep neural networks. In *International Conference on Machine Learning*, pages 10462–10472. PMLR, 2020.

[93] Tiankai Xie, Caleb Geniesse, Jiaqing Chen, Yaoqing Yang, Dmitriy Morozov, Michael W Mahoney, Ross Maciejewski, and Gunther H Weber. Evaluating loss landscapes from a topology perspective. *arXiv preprint arXiv:2411.09807*, 2024.

[94] Greg Yang and Edward J Hu. Feature learning in infinite-width neural networks. *arXiv preprint arXiv:2011.14522*, 2020.

[95] Zhifan Ye, Kejing Xia, Yonggan Fu, Xin Dong, Jihoon Hong, Xiangchi Yuan, Shizhe Diao, Jan Kautz, Pavlo Molchanov, and Yingyan Celine Lin. Longmamba: Enhancing mamba's long-context capabilities via training-free receptive field enlargement. In *The Thirteenth International Conference on Learning Representations*, 2025.

[96] Annan Yu, Chloé Becquey, Diana Halikias, Matthew Esmaili Mallory, and Alex Townsend. Arbitrary-depth universal approximation theorems for operator neural networks. *arXiv preprint arXiv:2109.11354*, 2021.

[97] Annan Yu, Dongwei Lyu, Soon Hoe Lim, Michael W Mahoney, and N Benjamin Erichson. Tuning frequency bias of state space models. *International Conference on Learning Representations*, 2025.

[98] Annan Yu, Michael W Mahoney, and N Benjamin Erichson. HOPE for a robust parameterization of long-memory state space models. *Internation Conference on Learning Representations*, 2025.

[99] Annan Yu, Arnur Nigmetov, Dmitriy Morozov, Michael W. Mahoney, and N. Benjamin Erichson. Robustifying state-space models for long sequences via approximate diagonalization. In *The Twelfth International Conference on Learning Representations*, 2024.

[100] Annan Yu, Yunan Yang, and Alex Townsend. Tuning frequency bias in neural network training with nonuniform data. *International Conference on Learning Representations*, 2023.

[101] Chulhee Yun, Srinadh Bhojanapalli, Ankit Singh Rawat, Sashank J Reddi, and Sanjiv Kumar. Are transformers universal approximators of sequence-to-sequence functions? *Internation Conference on Learning Representations*, 2020.

[102] Fengrui Zhang, Jiaoyi Hou, Dayong Ning, Cheng Zhou, Gangda Liang, and Zhilei Liu. Srs4: A stacked residual deep neural network for heave motion continuous prediction of salvage barge. *Available at SSRN 4938844*, 2024.

[103] Hanwei Zhang, Ying Zhu, Dan Wang, Lijun Zhang, Tianxiang Chen, Ziyang Wang, and Zi Ye. A survey on visual mamba. *Applied Sciences*, 14(13):5683, 2024.

[104] Guoqiang Zhong, Li-Na Wang, Xiao Ling, and Junyu Dong. An overview on data representation learning: From traditional feature learning to recent deep learning. *The Journal of Finance and Data Science*, 2(4):265–278, 2016.

[105] Ding-Xuan Zhou. Universality of deep convolutional neural networks. *Applied and computational harmonic analysis*, 48(2):787–794, 2020.

[106] Tian Zhou, Ziqing Ma, Qingsong Wen, Xue Wang, Liang Sun, and Rong Jin. Fedformer: Frequency enhanced decomposed transformer for long-term series forecasting. In *International Conference on Machine Learning*, pages 27268–27286. PMLR, 2022.

[107] Lianghui Zhu, Liao Bencheng, Qian Zhang, Xinlong Wang, Wenyu Liu, and Xinggang Wang. Vision mamba: Efficient visual representation learning with bidirectional state space model. *International Conference on Machine Learning*, 2024.

A Related works

Sequence Models. Sequential data appear across a wide range of domains, including natural language processing, computer vision, generative modeling, and scientific machine learning. To model such data, primitive deep learning approaches primarily relied on recurrent neural networks (RNNs) and their variants [6, 13, 22, 68, 55], as well as convolutional neural networks (CNNs) [9, 66]. The last decade has witnessed the dominance of the transformer architecture [37, 17, 41, 106, 54], following the seminal work [83]. Recently, a new class of models known as state-space models (SSMs) has emerged as a promising competitor [28, 27, 30, 77, 25, 20]. These models represent sequences through an underlying continuous-time dynamical system and offer a key advantage: they can handle sequences of varying lengths with a fixed number of parameters [85] and be trained with time and memory complexity that scales linearly with sequence length [28, 77, 25].

State Space Models. The term "state space models" (SSMs) originates from control theory and dates back to [36]. The first widely adopted SSM in machine learning was the S4 model proposed by [28]. Both the original S4 and its successor, Liquid-S4 [30], use a diagonal-plus-rank-one (DPRO) structure in the state matrix to significantly reduce computational cost compared to traditional RNNs. Later, [27] showed that a purely diagonal state matrix could achieve comparable performance, leading to the simplified S4D model. Since then, most SSMs have adopted diagonal state matrices, including S5 [77], Regularized SSM [46], Stable-SSM [86], S4-PTD, and S5-PTD [99, 63]. While a diagonal parameterization explores the structural simplicity of SSMs, [59] analyzes the computational acceleration of LTI systems and [12] investigates its numerical stability. Other works explore implicit sequence models that do not rely directly on an LTI formulation or rely on a modified LTI formulation, such as [98, 1, 56, 69]. An extensive list of different SSM architectures has been given in the survey articles [89, 58]. The expressiveness of SSMs has been studied in [98, 47], their training dynamics in [76, 97], and generalization properties in [97, 46]. Several studies have also investigated the representation stability of SSMs, including [86, 98]. Applications of SSMs in different scientific fields have been studied in several papers [102, 90, 63].

Mamba Models. Mamba [25] extends SSMs by introducing input-dependent dynamics via a selective mechanism, resulting in a highly efficient sequential architecture. Unlike earlier SSMs that use fixed, input-independent recurrence, Mamba adapts its dynamics at each step, enabling it to rival transformer-based models in language tasks. The theoretical benefits of this input-dependent recurrence was studied in [53] through the lens of controlled differential equations (CDEs). Mamba has since inspired a number of extensions and studies. Mamba2 [20] incorporates a multihead structure with softmax gating. Mamba has also been applied beyond language modeling [58], including computer vision [107, 103, 44], time-series forecasting [91], multimodal learning [62], and audio processing [43]. In addition, [51] proposed using Mamba as a foundation model backbone across modalities. Despite its versatility, follow-up studies such as [3] have highlighted the limitations of Mamba on long-range sequence benchmarks such as LRA. The S7 model [79] has been proposed as another selective model with slightly improved performances on LRA tasks; though, the accuracies are still substantially worse than models like S4D and S5. Other efforts to enhance Mamba's long memory retention and selectivity mechanism are found in [95] and [65], respectively. The spectral properties of the state matrix are considered in [24] and related to Mamba's state-tracking capabilities. In addition, the recent work [32] proposes a theoretical generalization upper bound based on the Rademacher complexity of Mamba models. Notably, [74] conducted a thorough comparison of these different recurrent units, including S4, Mamba, and traditional RNNs. Many works have shown the advantages of a bidirectional structure in SSMs and Mambas [34, 48], which we also adopt in training the LRA benchmark tasks.

Universal Approximation Theorems. In this paper, we use the universal approximation theorem (UAT) as a tool to assess a model's expressiveness. UATs ask whether a target function can be approximated to arbitrary accuracy by a sufficiently large neural network. This line of work dates back to [18], who proved that two-layer neural networks with sigmoid activation are universal approximators. This result was later extended to networks with any continuous, non-polynomial activation function. While many classical results focus on shallow but wide networks, recent work by [39] established that deep, narrow networks can also be universal approximators. Universal approximation properties have been studied across various architectures. Notable examples include shallow and wide operator neural networks [50, 15], as well as their deep and narrow counterparts [96]. For sequence models, UATs are known for RNNs [71], CNNs [105], Transformers [101], and

SSMs [86]. There are limited works on the universal approximation properties of Mamba models. One notable exception is [53], where the uniform closure of Mamba (i.e., functions that can be uniformly approximated by Mamba) is analyzed in a continuous setting (i.e., the inputs are continuous time series instead of discrete sequences) through linear controlled differential equations. The analysis there highlights the important role of an input-dependent sampling interval Δ in the expressiveness of Mamba, suggesting that Theorem 1 may not hold for a trainable Δ (see Appendix G).

Width and Depth of Neural Networks. While UATs focus on the density of neural networks in a given topology, more practically relevant questions involve the rate of approximation, e.g., how deep or wide a network must be to approximate a target function within a given accuracy. One of the most celebrated results is by [82], which shows that depth improves expressiveness more efficiently than width. However, in practice, deep but narrow networks often face optimization challenges during training [23, 57, 16, 67]. In contrast, networks with greater effective width tend to enjoy better theoretical guarantees on generalization. This advantage can be understood through both the neural tangent kernel (NTK) perspective [35, 7, 2, 11, 100] and mean-field theory [52, 80, 10], both of which highlight the benefits of wide models in training dynamics and generalization performance.

Sensitivity Analysis. Neural networks often operate on high-dimensional inputs, and a large body of work has studied how to quantify the sensitivity of the output to individual input components — a line of research typically referred to as attribution. While our paper focuses on relative gradients, many other gradient-based attribution methods have been developed, including DeepLIFT [73], integrated gradients [81], sensitivity-n [4], and others [8, 75]. Most of these methods compare a given input to a baseline or reference input, whereas our analysis focuses specifically on the effect of large-magnitude inputs in isolation without reference to a benchmark input.

Training Stability and the Loss Landscape. Training stability in deep neural networks has been extensively studied through the lens of loss landscape geometry. Sharp minima and high-curvature regions are often associated with poor generalization and unstable optimization [38, 14, 42]. Gradient explosion or vanishing can lead to optimization failure [23, 57] for recurrent neural networks. More recent works have linked curvature and gradient dynamics to the trainability of neural networks [16, 67, 70]. These studies emphasize the importance of smooth, well-conditioned landscapes for stable training, motivating architectural choices [31, 93] and learning rate schedulers [49] that mitigate instability.

B Proofs of UAT and non-UAT results

In this section, we prove all technical results related to UATs presented in section 3 and 6. Recall that the univariate neural network architecture that we study in this paper is given by

$$\tilde{G}(\mathbf{u}) = \tilde{G}((u_1, \dots, u_L)) = \mathbf{N}\sigma(\Gamma((\mathbf{M}u_1, \dots, \mathbf{M}u_L))_L + \boldsymbol{\theta}).$$

A pictorial illustration of this architecture is given in Figure 5.

B.1 Proof of Theorem 1

To prove that such a $\tilde{G}$ is not a universal approximator when $\Gamma = \Gamma_{\text{S6}}$, we will see that since an S6 model ties the matrices $\overline{\mathbf{B}}_k$ and $\overline{\mathbf{C}}_k$ for all channels, the system becomes a quadratic encoder of the input sequence. We need the following technical lemma to show that a quadratic encoder is not invertible, and therefore, information will be lost when we apply this encoder to an input sequence.

Lemma 1. Given any $L \geq 3$, there exists a continuous function $G : [0,1]^L \to \mathbb{R}$ such that given any quadratic polynomial of L variables $P : [0,1]^{L-1} \times \{1\} \to \mathbb{R}$, there exist two points $\mathbf{x}, \mathbf{y} \in [0,1]^{L-1} \times \{1\}$ such that

$$P(\mathbf{x}) = P(\mathbf{y}), \qquad |G(\mathbf{x}) - G(\mathbf{y})| > 1.$$

Proof. Since the restriction of a quadratic polynomial of L variables to 3 variables is still a quadratic polynomial, without loss of generality, we assume that $L = 3$. Moreover, instead of assuming that G and P are functions on $[0,1]^{3-1} \times \{1\}$, we can assume that they are functions on $[0,1]^2$. It is well-known that there is a number $N \geq 1$ such that every bivariate quadratic polynomial has at most N strict local minima or maxima. We construct G by selecting $N+1$ arbitrary distinct points $\mathbf{x}_1, \mathbf{x}_2, \dots, \mathbf{x}_{N+1}$ in $(0,1)^2$. Around each point $\mathbf{x}_j$, we make a small disk $D_j = D_\rho(\mathbf{x}_j)$.

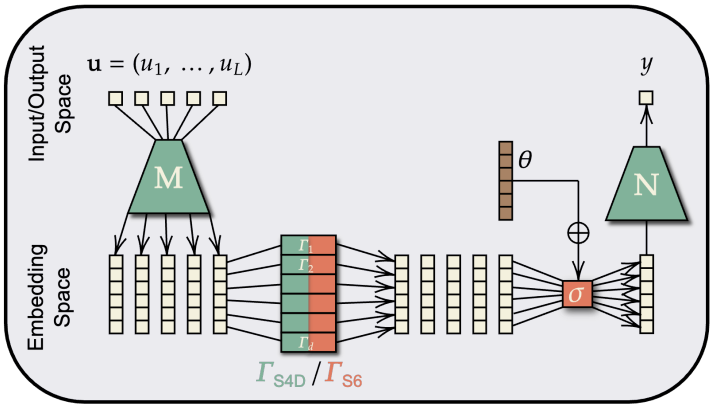

Figure 5: The architecture of the neural network eq. (5) that we study in this paper. In this picture, a horizontal operator is applied channel-wise to every sequence in a channel, and a vertical operation is applied element-wise to every position in a sequence. A green color indicates a linear operator while an orange color indicates a nonlinear one.

By taking ρ small enough, we can also ensure that $D_j \subset [0,1]^2$ for all $1 \leq j \leq N+1$ and that $D_1, D_2, \ldots, D_{N+1}$ are mutually disjoint. Let G be a continuous function such that $G(\mathbf{x}_j) = 0$ for every $1 \leq j \leq N+1$ and G equals 2 on ∂D_j, the boundary of D_j, for every $1 \leq j \leq N+1$. Such a G clearly exists by Urysohn's lemma. We claim that G satisfies the condition in the our lemma. To see this, given any arbitrary quadratic polynomial $P : [0,1]^2 \to \mathbb{R}$, we let S_j be the connected component of the set $\{\mathbf{x} | P(\mathbf{x}) = P(\mathbf{x}_j)\}$ that contains $\mathbf{x}_j$. There are two possibilities: either S_j intersects ∂D_j or not. If S_j does not intersect ∂D_j, then that means there is a strict local minimum or a strict local maximum of P in D_j, but $D_1, \ldots, D_{N+1}$ are mutually disjoint and there are at most N local minima or maxima of P. Hence, there is at least one j such that S_j intersects ∂D_j. Let $\mathbf{y} \in S_j \cap \partial D_j$. Then, we have that

$$P(\mathbf{x}_j) = P(\mathbf{y}), \qquad |G(\mathbf{x}_j) - G(\mathbf{y})| = |0 - 2| > 1.$$

The proof is complete. □

We are now ready to prove Theorem 1. The proof of the first part is built upon a result from [60] for UAT of a two-layer wide neural network to approximate any continuous function and a result from [88] for UAT of LTI systems to approximate any convolutional kernel.

Proof of Theorem 1. We prove the two statements separately.

Proof of Part I. Without loss of generality, assume that σ is 1-Lipschitz.[4] Let a continuous function $G : [0,1]^L \to \mathbb{R}$ and an error tolerance $\epsilon > 0$ be given. By [60], there exists a function $\tilde{G} : [0,1]^L \to \mathbb{R}$ of the form

$$\tilde{G}(\mathbf{u}) = \sum_{i=1}^{d} f^{(i)} \sigma((\mathbf{w}^{(i)})^\top \mathbf{u} + \theta^{(i)}),$$

where $\mathbf{w}^{(i)} \in \mathbb{R}^L$ and $b_i \in \mathbb{R}$ for every $1 \leq i \leq d$, such that

$$|\tilde{G}(\mathbf{u}) - G(\mathbf{u})| \leq \frac{\epsilon}{2}$$

for every $\mathbf{u} \in [0,1]^L$. For any $1 \leq i \leq d$, by [87], there exist $n_i \geq 1$, $\mathbf{A}^{(i)} \in \mathbb{R}^{n_i \times n_i}$, $\mathbf{B}^{(i)} \in \mathbb{R}^{n_i \times 1}$, and $\mathbf{C}^{(i)} \in \mathbb{R}^{1 \times n_i}$, such that the matrices $\overline{\mathbf{A}}^{(i)}$, $\overline{\mathbf{B}}^{(i)}$, and $\overline{\mathbf{C}}^{(i)}$ from the discretized LTI system (see eq. (2)) satisfy that

$$|(\mathbf{w}_j)^{(i)} - \overline{\mathbf{C}}^{(i)} (\overline{\mathbf{A}}^{(i)})^{L-j} \overline{\mathbf{B}}^{(i)}| < \frac{\epsilon}{2\sqrt{d} L (\|\mathbf{f}\|_2 + 1)}$$

[4] Otherwise, if σ is ℓ-Lipschitz, we can divide σ by ℓ to make it 1-Lipschitz and multiply $\mathbf{N}$ by ℓ so that the value of $\tilde{G}$ does not change.

for all $1 \leq j \leq L$, where $\mathbf{f} = [f^{(1)} \ \cdots \ f^{(d)}]^\top$. Hence, we have that

$$\begin{aligned}
&\left|\sigma((\mathbf{w}^{(i)})^\top \mathbf{u} + \theta^{(i)}) - \sigma\left(\sum_{j=1}^{L} \overline{\mathbf{C}}^{(i)} (\overline{\mathbf{A}}^{(i)})^{L-j} \overline{\mathbf{B}}^{(i)} u_j + \theta^{(i)}\right)\right| \\
&\quad \leq \left|(\mathbf{w}^{(i)})^\top \mathbf{u} - \left(\sum_{j=1}^{L} \overline{\mathbf{C}}^{(i)} (\tilde{\mathbf{A}}^{(i)})^{L-j} \overline{\mathbf{B}}^{(i)} u_j\right)\right| \\
&\quad \leq \sqrt{\sum_{j=1}^{L} \left((\mathbf{w}^{(i)})_j - \overline{\mathbf{C}}^{(i)} (\overline{\mathbf{A}}^{(i)})^{L-j} \overline{\mathbf{B}}^{(i)}\right)^2} \, \|\mathbf{u}\|_2 \leq L \frac{\epsilon}{2\sqrt{d} L (\|\mathbf{f}\|_2 + 1)} = \frac{\epsilon}{2\sqrt{d}(\|\mathbf{f}\|_2 + 1)},
\end{aligned}$$

where the first inequality follows from the Lipschitz continuity of σ and the second inequality follows from the Hölder's inequality. Set $n = \sum_{i=1}^{d} n_i$ and define a block-diagonal matrix $\mathbf{A}$ so that

$$\mathbf{A} = \begin{bmatrix} \mathbf{A}^{(1)} & & & \\ & \mathbf{A}^{(2)} & & \\ & & \ddots & \\ & & & \mathbf{A}^{(d)} \end{bmatrix}.$$

For every $1 \leq i \leq d$, define $\mathbf{B}^{(i)} \in \mathbb{R}^{n \times 1}$ to be a sparse column vector so that $\mathbf{B}^{(i)}((\sum_{i'=1}^{i-1} n_{i'} + 1) : (\sum_{i'=1}^{i} n_{i'})) = \mathbf{B}^{(i)}$ and is zero elsewhere. Similarly, define $\mathbf{C}^{(i)} \in \mathbb{R}^{1 \times n}$ to be a sparse column vector so that $\mathbf{C}^{(i)}((\sum_{i'=1}^{i-1} n_{i'} + 1) : (\sum_{i'=1}^{i} n_{i'})) = \mathbf{C}^{(i)}$ and is zero elsewhere. Now, it is easy to see that given these definitions, the S4D defined in eq. (1) satisfies that

$$(\mathbf{\Gamma}_{\text{S4D}}((u_1, \ldots, u_L))_L)^{(i)} = \sum_{j=1}^{L} \overline{\mathbf{C}}^{(i)} (\overline{\mathbf{A}}^{(i)})^{L-j} \overline{\mathbf{B}}^{(i)} u_j$$

for every $1 \leq i \leq d$. Hence, let $\tilde{G}_{\text{S4D}}$ be such that

$$\tilde{G}_{\text{S4D}} : [0,1]^L \to \mathbb{R}, \quad (u_1, \ldots, u_L) \mapsto \mathbf{f}\sigma(\mathbf{\Gamma}_{\text{S4D}}((\mathbf{M}u_1, \ldots, \mathbf{M}u_L))_L + \boldsymbol{\theta}),$$

where $\mathbf{M} = [1 \ \cdots \ 1]^\top$. For any $\mathbf{u} \in \mathbb{R}^L$, we have that

$$\begin{aligned}
|\tilde{G}_{\text{S4D}}(\mathbf{u}) - \tilde{G}(\mathbf{u})| &\leq \|\mathbf{f}\|_2 \sqrt{\sum_{i=1}^{d} \left(\sigma((\mathbf{w}^{(i)})^\top \mathbf{u}) - \sigma\left(\sum_{j=1}^{L} \overline{\mathbf{C}}^{(i)} (\overline{\mathbf{A}}^{(i)})^{L-j} \overline{\mathbf{B}}^{(i)} u_j\right)\right)^2} \\
&\leq \|\mathbf{f}\|_2 \sqrt{d} \frac{\epsilon}{2\sqrt{d}(\|\mathbf{f}\|_2 + 1)} < \frac{\epsilon}{2}.
\end{aligned}$$

Now, for any $\mathbf{u} \in \mathbb{R}^L$, we have that

$$|\tilde{G}_{\text{S4D}}(\mathbf{u}) - G(\mathbf{u})| \leq |\tilde{G}_{\text{S4D}}(\mathbf{u}) - \tilde{G}(\mathbf{u})| + |\tilde{G}(\mathbf{u}) - G(\mathbf{u})| \leq \frac{\epsilon}{2} + \frac{\epsilon}{2} \leq \epsilon.$$

The statement is proved.

Proof of Part II. Given any sequence $\mathbf{u} \in \mathbb{R}^L$, any encoder $\mathbf{M} = [m^{(1)} \ \cdots \ m^{(L)}]^\top$, and any Mamba parameters $\mathbf{A} \in \mathbb{R}^{n \times n}$, $\mathbf{B} \in \mathbb{R}^{n \times d}$, and $\mathbf{C} \in \mathbb{R}^{d \times n}$, we first show how the Mamba system in eq. (3) can be simplified. For any $1 \leq i \leq d$, we have that

$$\begin{aligned}
\mathbf{x}_{k+1}^{(i)} &= \mathbf{A}\mathbf{x}_k^{(i)} + (\overline{\mathbf{P}} u_k) m^{(i)} u_k, \\
(\mathbf{y}_k)^{(i)} &= (u_k \overline{\mathbf{Q}}) \mathbf{x}_k^{(i)},
\end{aligned} \tag{9}$$

where $\overline{\mathbf{A}} = \exp(\mathbf{A})$, $\mathbf{P} = \mathbf{A}^{-1}(\overline{\mathbf{A}} - \mathbf{I})\mathbf{B}\mathbf{M}$, and $\overline{\mathbf{Q}} = \mathbf{M}^\top \mathbf{C}$ are fixed matrices depending only on $\mathbf{A}$, $\mathbf{B}$, $\mathbf{C}$, and $\mathbf{M}$. Hence, the ith entry of the final output is given by

$$\mathbf{\Gamma}_{\text{S6}}((\mathbf{M}u_1, \ldots, \mathbf{M}u_L))_L^{(i)} = m^{(i)} \underbrace{u_L \left(\sum_{j=1}^{L} \overline{\mathbf{Q}} \, \overline{\mathbf{A}}^{L-j} \, \overline{\mathbf{P}} u_j^2\right)}_{F((u_1, \ldots, u_L))}.$$

Importantly, note that since $u_L = 1$, F is a quadratic function in $u_1, \dots, u_L$ that does not depend on i. The output of $\tilde{G}_{\text{S6}}$ can then be expressed as

$$\tilde{G}_{\text{S6}}(\mathbf{u}) = \sum_{i=1}^{d} n^{(i)} \sigma(m^{(i)} F(\mathbf{u}) + \theta_i),$$

where $\mathbf{N} = [n^{(1)} \ \cdots \ n^{(L)}]$. Let G be the function defined in Lemma 1. Then, given any choice of $\mathbf{M}, \mathbf{N}, \boldsymbol{\theta}, \mathbf{A}, \mathbf{B}$, and $\mathbf{C}$, we know that there is a pair of inputs $\mathbf{u}$ and $\mathbf{v}$ such that

$$F(\mathbf{u}) = F(\mathbf{v}), \qquad |G(\mathbf{u}) - G(\mathbf{v})| > 1.$$

Since $F(\mathbf{u}) = F(\mathbf{v})$, we also have that $\tilde{G}_{\text{S6}}(\mathbf{u}) = \tilde{G}_{\text{S6}}(\mathbf{v})$. By the triangle inequality, we have

$$|G(\mathbf{u}) - \tilde{G}_{\text{S6}}(\mathbf{u})| + |G(\mathbf{v}) - \tilde{G}_{\text{S6}}(\mathbf{v})| \geq |G(\mathbf{u}) - G(\mathbf{v})| > 1.$$

Setting $\epsilon = 1/2$, we are done. □

B.2 Proof of Theorem 4

The proof of Theorem 4 can be easily established upon our proof that S4D models are universal approximators.

Proof of Theorem 4. Note that the construction of a universal approximator in Theorem 1 can be achieved by using the same $\mathbf{C}^{(i)} = [1 \quad \cdots \quad 1]$ for all $1 \leq i \leq d$ (see [88, 97]). The second statement follows immediately from the first statement of Theorem 1 by setting ${}^1\mathbf{B}_{\text{weight}} = \mathbf{0}$, $\mathbf{B}^{(i)}_{\text{bias}}$ to be the same $\mathbf{B}^{(i)}$ used in Γ_{S4D}, and ${}^1\mathbf{C}$ to be the rank-1 matrix whose entries are all d^{-1} so that $u_L \mathbf{M}^\top {}^1\mathbf{C} = [1 \quad \cdots \quad 1]$. For the first statement, consider the function $H(\mathbf{u})$ given by $H(\mathbf{u}) = G(\sqrt{\mathbf{u}})$, where the square-root is applied elementwise. Clearly, H is continuous since G is continuous. Then, we know, by the second statement, that there exist $\mathbf{M} = [1 \quad \cdots \quad 1]^\top, \mathbf{N}, \boldsymbol{\theta}, \tilde{\mathbf{A}}, {}^1\tilde{\mathbf{B}}_{\text{weight}} = \mathbf{0}, \tilde{\mathbf{B}}^{(i)}_{\text{bias}}$, and ${}^1\tilde{\mathbf{C}} = [1/d]_{i,j}$ such that the B_2S_6 system $\tilde{\mathbf{\Gamma}}_{\text{B}_2\text{S}_6}$ defined in eq. (7) with $h = 1$ and $p = d$ and the map

$$\tilde{H}_{\text{B}_2\text{S}_6} : [0,1]^L \to \mathbb{R}, \quad (u_1, \dots, u_L) \mapsto \mathbf{N}\sigma(\tilde{\mathbf{\Gamma}}_{\text{B}_2\text{S}_6}((\mathbf{M}u_1, \dots, \mathbf{M}u_L))_L + \boldsymbol{\theta})$$

satisfy that

$$|\tilde{H}_{\text{B}_2\text{S}_6}(\mathbf{u}) - H(\mathbf{u})| \leq \epsilon, \qquad \text{for any } \mathbf{u} \in [0,1]^{L-1} \times \{1\}.$$

Now, define $h = d$ and $p = 1$. Let $\mathbf{M}, \mathbf{N}, \boldsymbol{\theta}, \mathbf{A} = \tilde{\mathbf{A}}$ be the same matrices, and let ${}^j\mathbf{B}_{\text{weight}} = \tilde{\mathbf{B}}^{(j)}_{\text{bias}}$, $\mathbf{B}^{(i)}_{\text{bias}} = \mathbf{0}$, and ${}^j\mathbf{C} = [1 \quad \cdots \quad 1]$ for all i and j. Then, it is clear that the system $\mathbf{\Gamma}_{\text{B}_2\text{S}_6}$ defined by these matrices satisfies that

$$(\mathbf{\Gamma}_{\text{B}_2\text{S}_6}(\mathbf{u}))_L = (\tilde{\mathbf{\Gamma}}_{\text{B}_2\text{S}_6}(\mathbf{u}^2))_L, \qquad \text{for any } \mathbf{u} \in [0,1]^{L-1} \times \{1\},$$

where $\mathbf{u}^2$ is the sequence obtained by squaring every entry of $\mathbf{u}$. Hence, the map

$$\tilde{G}_{\text{B}_2\text{S}_6} : [0,1]^{L-1} \times \{1\} \to \mathbb{R}, \quad (u_1, \dots, u_L) \mapsto \mathbf{N}\sigma(\mathbf{\Gamma}_{\text{B}_2\text{S}_6}((\mathbf{M}u_1, \dots, \mathbf{M}u_L))_L + \boldsymbol{\theta})$$

satisfies that

$$|\tilde{G}_{\text{B}_2\text{S}_6}(\mathbf{u}) - G(\mathbf{u})| = |\tilde{H}_{\text{B}_2\text{S}_6}(\mathbf{u}^2) - H(\mathbf{u}^2)| \leq \epsilon, \qquad \text{for any } \mathbf{u} \in [0,1]^{L-1} \times \{1\}.$$

The proof is complete. □

C Proofs of inductive bias results

In this section, we prove Theorem 2 and 5. The proof of these results relies on a very simple argument that helps us avoid the cancellation of terms, which we state below.

Lemma 2. Let $p \in \mathbb{R}$ be given. Assume $f : \mathbb{R} \to \mathbb{R}$ and $g : \mathbb{R} \to \mathbb{R}$ are two functions such that $f(x) = \alpha x^p + o(x^p)$ and $g(x) = \beta x^p + o(x^p)$ as $x \to \infty$, for some constants $\alpha, \beta \neq 0$. Then, we have that for a.e. choice of $c_1, c_2 \in \mathbb{R}$ that $c_1 f(x) + c_2 g(x) = \gamma x^p + o(x^p) = \Theta(x^p)$ as $x \to \infty$ for some $\gamma \neq 0$.

Proof. The proof is straightforward: as long as we have that $\alpha c_1 + \beta c_2 \neq 0$, the conclusion is satisfied. Since α and β are nonzero, the equation $\alpha c_1 + \beta c_2 = 0$ is satisfied only on a Lebesgue null set of c_1 and c_2. □

C.1 Proof of Theorem 2

We now prove the main theorems by explicitly calculating the Jacobians.

Proof of Theorem 2. Given an S6 system in eq. (3) and an input sequence $\mathbf{u} = (\mathbf{u}_1, \ldots, \mathbf{u}_L)$, let $\mathbf{y}_L = \Gamma_{\text{S6}}(\mathbf{u})$ be the last output of the system. For any $1 \le s \le d$, we have that

$$y_L^{(s)} = \mathbf{u}_L^\top \mathbf{C}\mathbf{x}_L = \mathbf{u}_L^\top \mathbf{C} \sum_{j=1}^{L} \left(\prod_{i=j+1}^{L} \mathbf{A}(\mathbf{u}_i) \right) \mathbf{B}(\mathbf{u}_j) u_j^{(s)},$$

where

$$\mathbf{A}(\mathbf{u}_i) = \exp\left(\Delta(\mathbf{u}_i)\mathbf{A}\right) = \exp\left(\text{softplus}(\mathbf{w}^\top \mathbf{u}_i)\mathbf{A}\right),$$
$$\mathbf{B}(\mathbf{u}_i) = \mathbf{A}^{-1}\left(\exp\left(\text{softplus}(\mathbf{w}^\top \mathbf{u}_i)\mathbf{A}\right) - \mathbf{I}\right)\mathbf{B}\mathbf{u}_i.$$

Note that we have changed the notations so that $\mathbf{A}(\mathbf{u}_i)$ is exactly the matrix $\overline{\mathbf{A}}_i$ and $\mathbf{B}(\mathbf{u}_i)$ is exactly the matrix $\overline{\mathbf{B}}_i$ in eq. (3). This helps us better keep track of the dependency of every term on the input $\mathbf{u}$. In addition, it is easy to see that $b^{(i)}$ does not play a role in the asymptotic behaviors when $c \to \pm\infty$. Hence, we set them to zero. For any s, we have

$$(\mathbf{J}_r)_{s,s} = \frac{\partial y_L^{(s)}}{\partial u_r^{(s)}} = \mathbf{u}_L^\top \mathbf{C} \sum_{j=1}^{L} \underbrace{\frac{\partial}{\partial u_r^{(s)}} \left[\left(\prod_{i=j+1}^{L} \mathbf{A}(\mathbf{u}_i) \right) \mathbf{B}(\mathbf{u}_j) u_j^{(s)} \right]}_{\mathbf{d}_j^{(r,s)}},$$

where

$$\mathbf{d}_j^{(r,s)} = \begin{cases} \left[\frac{\partial}{\partial u_r^{(s)}} \mathbf{A}(\mathbf{u}_r)\right] \left(\prod_{i=j+1, i\neq r}^{L} \mathbf{A}(\mathbf{u}_i)\right) \mathbf{B}(\mathbf{u}_j) u_j^{(s)} & , \ j < r, \\ \left(\prod_{i=r+1}^{L} \mathbf{A}(\mathbf{u}_i)\right) \left(\mathbf{B}(\mathbf{u}_r) + u_r^{(s)} \frac{\partial}{\partial u_r^{(s)}} \mathbf{B}(\mathbf{u}_r)\right) & , \ j = r, \\ \mathbf{0} & , \ j > r. \end{cases}$$

For any $s \neq t$, we have

$$(\mathbf{J}_r)_{s,t} = \frac{\partial y_L^{(t)}}{\partial u_r^{(s)}} = \mathbf{u}_L \mathbf{C} \sum_{j=1}^{L} \underbrace{\frac{\partial}{\partial u_r^{(s)}} \left[\left(\prod_{i=j+1}^{L} \mathbf{A}(\mathbf{u}_i) \right) \mathbf{B}(\mathbf{u}_j) u_j^{(t)} \right]}_{\mathbf{f}_j^{(r,s,t)}},$$

where

$$\mathbf{f}_j^{(r,s,t)} = \begin{cases} \left[\frac{\partial}{\partial u_r^{(s)}} \mathbf{A}(\mathbf{u}_r)\right] \left(\prod_{i=j+1, i\neq r}^{L} \mathbf{A}(\mathbf{u}_i)\right) \mathbf{B}(\mathbf{u}_j) u_j^{(t)} & , \ j < r, \\ \left(\prod_{i=r+1}^{L} \mathbf{A}(\mathbf{u}_i)\right) u_r^{(t)} \frac{\partial}{\partial u_r^{(s)}} \mathbf{B}(\mathbf{u}_r) & , \ j = r, \\ \mathbf{0} & , \ j > r. \end{cases}$$

We now break the proof into two cases.

Case I: $c \to \infty$**.** We discuss the cases when $r < k$, $r = k$, and $r > k$ separately.

- When $r < k$, it is easy to check that $\|\mathbf{A}(\mathbf{u}_r)\|$ decays exponentially when $c \to \infty$. Hence, we have $\|\mathbf{d}_j^{(r,s)}\|$ and $\|\mathbf{f}_j^{(r,s,t)}\|$ decay exponentially as $c \to \infty$ for every s, t, and j. That is, the Jacobian norm $\|\mathbf{J}_r\|_F$ decays exponentially as $c \to \infty$.
- When $r = k$, the norm of the term

  $$\left(\prod_{i=r+1}^{L} \mathbf{A}(\mathbf{u}_i) \right) u_r^{(t)} \frac{\partial}{\partial u_r^{(s)}} \mathbf{B}(\mathbf{u}_r)$$

  grows like $\alpha c + o(c)$ as $c \to \infty$ for all $\mathbf{A}$ and a.e. choice of and $\mathbf{B}$, where $\alpha \neq 0$ is a constant. That is, $\mathbf{d}_k^{(k,s)}$ and $\mathbf{f}_k^{(k,s,t)}$ grow like a linear factor plus a $o(c)$ term as $c \to \infty$. Hence, by Lemma 2, for a.e. choice of $\mathbf{C}$, we have that $\|\mathbf{J}_k\|_F = \Theta(c)$ as $c \to \infty$.

- When $r > k$, it is straightforward to check that $\|\mathbf{d}_k^{(r,s)}\| = \alpha(s)c^2 + o(c^2)$ for some constants $\alpha(s) \neq 0$ and a.e. choice of $\mathbf{B}$ and $\|\mathbf{f}_k^{(r,s,t)}\| = \beta(s,t)c^2 + o(c^2)$ for some constants $\beta(s,t) \neq 0$ and a.e. choice of $\mathbf{B}$. Hence, by Lemma 2, for a.e. choice of $\mathbf{C}$, we have that $\|\mathbf{J}_r\|_F = \Theta(c^2)$ as $c \to \infty$.

The first part of the theorem is proved by combining the three statements above.

Case II: $c \to -\infty$**.** We discuss the cases when $r < k$, $r = k$, and $r > k$ separately.

- When $r < k$, the only thing that changes in the expression of $\mathbf{J}_r$ when $c \to -\infty$ is the matrix $\mathbf{A}(\mathbf{u}_k)$, in which case it converges to $\mathbf{I}$. Hence, we have that $\|\mathbf{J}_r\|_F = \Theta(1)$.
- When $r = k$, we have that

$$\left\| \frac{\partial}{\partial u_k^{(s)}} \mathbf{A}(u_k) \right\| = \mathcal{O}(|c|^{-p})$$

  for any $p > 0$ and s. Moreover, we also have that

$$\|\mathbf{B}(\mathbf{u}_k)\| = \mathcal{O}(|c|^{-p}), \qquad \left\| \frac{\partial}{\partial u_k^{(s)}} \mathbf{B}(u_k) \right\| = \mathcal{O}(|c|^{-p}),$$

  for any $p > 0$ and s. That means we have $\|\mathbf{d}_j^{(k,s)}\|$ and $\|\mathbf{f}_j^{(k,s,t)}\|$ decay exponentially for any choice of s, t, and j. Hence, we have that $\|\mathbf{J}_k\|_F = \Theta(|c|^{-p})$ for any $p > 0$.
- When $r > k$, we note that while $\|\mathbf{u}_k\|$ grows linearly, the norm of the vector $\|\mathbf{B}(\mathbf{u}_k)\|$ decays exponentially. Therefore, we have that $\|\mathbf{B}(\mathbf{u}_k)u_k^{(s)}\|$ decays exponentially for every s. This shows that for a.e. $\mathbf{B}$, the norms $\|\mathbf{d}_j^{(r,s)}\|$ and $\|\mathbf{f}_j^{(r,s,t)}\|$ converge to constants for all s, t, and j. By Lemma 2, we have $\|\mathbf{J}_r\|_F = \Theta(1)$ for a.e. choice of $\mathbf{C}$.

The second part of the theorem is proved by combining the three statements above. The claim about an Γ_{S4D} system is obvious since the system is linear. □

Interestingly, from the proof of Theorem 2, we see that when $c \to \infty$, the reason why $S_{\text{S6},k}$ is large for $k > k_0$ is that $\mathbf{u}_k$ plays an important role in determining the matrix $\overline{\mathbf{B}}_{k_0}$ that affects a large input $\mathbf{u}_{k_0}$. This is analogous to the function $f(x, y) = xy$. When x is large and y is small, the gradient $(\partial/\partial x)f$ is still small but $(\partial/\partial y)f$ is huge.

C.2 Proof of Theorem 5

Once Theorem 2 is proved, the proof of Theorem 5 can be maintained easily from it.

Proof of Theorem 5. For each $1 \leq r \leq L$, the Jacobian $\mathbf{J}_r$ is a block diagonal matrix $\mathbf{J}_r = \text{diag}({}^1\mathbf{J}_r, \ldots, {}^h\mathbf{J}_r)$, where every ${}^j\mathbf{J}_r$ is a $p \times p$ matrix. Since the cases when c is negative and when c is positive are symmetric, without loss of generality, we assume that $c \to \infty$. We study the Jacobian norms when $r < k$, $r = k$, and $r > k$ separately. The following statements hold for a.e. model parameters.

- When $r < k$, from the proof of Theorem 2, we know that $\|{}^j\mathbf{J}_r\|$ decays exponentially when ${}^j\mathbf{w}^\top {}^j\mathbf{u} > 0$ and $\|{}^j\mathbf{J}_r\| = \Theta(1)$ when ${}^j\mathbf{w}^\top {}^j\mathbf{u} < 0$. Hence, by our assumption, we know that $\|\mathbf{J}_r\|_F = \Theta(1)$.
- When $r = k$, from the proof of Theorem 2, we know that $\|{}^j\mathbf{J}_r\| = \Theta(c)$ as long as ${}^j\mathbf{w}^\top {}^j\mathbf{u} > 0$. Hence, we have $\|\mathbf{J}_r\|_F = \Theta(c)$.
- When $r > k$, from the proof of Theorem 2, we know that $\|{}^j\mathbf{J}_r\| = \Theta(c^2)$ as long as ${}^j\mathbf{w}^\top {}^j\mathbf{u} > 0$. Hence, we have $\|\mathbf{J}_r\|_F = \Theta(c^2)$.

Combining the three cases, we proved the result. □

D Proof of the stability result

We now bring in the last piece of technical details by proving the stability result in Theorem 3. The proof again relies on a tedious expansion of the gradients, which then gives us expressions that are intellectually interesting to analyze with basic probability theory.

Proof of Theorem 3. Since we assumed that $d = 1$, we drop all superscripts for channel indices. Given an input $\mathbf{u} = (u_1, \dots, u_L)$ be an input and denote by $y_{\text{S4D}} = \Gamma_{\text{S4D}}(\mathbf{u})_L$ and $y_{\text{S6}} = \Gamma_{\text{S6}}(\mathbf{u})_L$ the outputs of an S4D system and an S6 system, respectively. Then, we have

$$\frac{\partial y_{\text{S4D}}}{\partial b} = \mathbf{C} \sum_{j=1}^{L} \underbrace{\frac{\partial}{\partial b} \left[\left(\prod_{i=j+1}^{L} \overline{\mathbf{A}} \right) \overline{\mathbf{B}} u_j \right]}_{\mathbf{r}_j},$$

where

$$\overline{\mathbf{A}} = \exp(\exp(b)\mathbf{A}), \qquad \overline{\mathbf{B}} = \mathbf{A}^{-1}(\overline{\mathbf{A}} - \mathbf{I})\mathbf{B},$$

and

$$\frac{\partial y_{\text{S6}}}{\partial w} = u_L \mathbf{C} \sum_{j=1}^{L} \underbrace{\frac{\partial}{\partial w} \left[\left(\prod_{i=j+1}^{L} \mathbf{A}(u_i) \right) \mathbf{B}(u_j) u_j \right]}_{\mathbf{s}_j},$$

$$\frac{\partial y_{\text{S6}}}{\partial b} = u_L \mathbf{C} \sum_{j=1}^{L} \underbrace{\frac{\partial}{\partial b} \left[\left(\prod_{i=j+1}^{L} \mathbf{A}(u_i) \right) \mathbf{B}(u_j) u_j \right]}_{\mathbf{t}_j},$$

where

$$\mathbf{A}(u_j) = \tilde{\mathbf{A}} = \exp(\text{softplus}(b)\mathbf{A}), \qquad \mathbf{B}(u_j) = \mathbf{A}^{-1}(\mathbf{A}(u_j) - \mathbf{I})\mathbf{B}u_j.$$

Note that the matrix $\mathbf{A}(u_j)$ does not really depend on u_j because we assumed that $w = 0$, but we keep the notation consistent with the proof of Theorem 2. In particular, we have that

$$\frac{\partial}{\partial b}\overline{\mathbf{A}} = \overline{\mathbf{A}}\mathbf{A}\exp(b), \qquad \frac{\partial}{\partial b}\overline{\mathbf{B}} = \mathbf{A}^{-1}\overline{\mathbf{A}}\mathbf{A}\exp(b)\mathbf{B} = \overline{\mathbf{A}}\mathbf{B}\exp(b).$$

and

$$\frac{\partial}{\partial w}\mathbf{A}(u) = \frac{\exp\left(\text{softplus}(b)\mathbf{A}\right)\mathbf{A}u}{1+e^{-b}}, \qquad \frac{\partial}{\partial w}\mathbf{B}(u) = \frac{\exp\left(\text{softplus}(b)\mathbf{A}\right)\mathbf{A}u}{1+e^{-b}}\mathbf{A}^{-1}\mathbf{B}u,$$
$$\frac{\partial}{\partial b}\mathbf{A}(u) = \frac{\exp\left(\text{softplus}(b)\mathbf{A}\right)\mathbf{A}}{1+e^{-b}}, \qquad \frac{\partial}{\partial b}\mathbf{B}(u) = \frac{\exp\left(\text{softplus}(b)\mathbf{A}\right)\mathbf{A}}{1+e^{-b}}\mathbf{A}^{-1}\mathbf{B}u.$$

Using the product rule, we can compute $\mathbf{r}_j$, $\mathbf{s}_j$, and $\mathbf{t}_j$:

$$\begin{aligned}
\mathbf{r}_j &= u_j \left(\overline{\mathbf{A}}^{L-j} \frac{\partial}{\partial b}\overline{\mathbf{B}} + \sum_{i=j+1}^{L} \left(\frac{\partial}{\partial b}\overline{\mathbf{A}} \right) \overline{\mathbf{A}}^{L-j-1}\overline{\mathbf{B}} \right) \\
&= \overline{\mathbf{A}}^{L-j-1} u_j \left(\overline{\mathbf{A}} \frac{\partial}{\partial b}\overline{\mathbf{B}} + \left(\sum_{i=j+1}^{L} \frac{\partial}{\partial b}\overline{\mathbf{A}} \right) \overline{\mathbf{B}} \right) \\
&= \overline{\mathbf{A}}^{L-j} u_j \exp(b) \left(\overline{\mathbf{A}} + (L-j)(\overline{\mathbf{A}} - \mathbf{I}) \right) \mathbf{B},
\end{aligned}$$

and

$$\begin{aligned}
\mathbf{s}_j &= u_j \left(\tilde{\mathbf{A}}^{L-j} \frac{\partial}{\partial w} \mathbf{B}(u_j) + \sum_{i=j+1}^{L} \frac{\partial}{\partial w} \mathbf{A}(u_i) \tilde{\mathbf{A}}^{L-j-1} \mathbf{B}(u_j) \right) \\
&= \tilde{\mathbf{A}}^{L-j-1} \left(u_j \, \tilde{\mathbf{A}} \, \frac{\partial}{\partial w} \mathbf{B}(u_j) + u_j \left(\sum_{i=j+1}^{L} \frac{\partial}{\partial w} \mathbf{A}(u_i) \right) \mathbf{B}(u_j) \right) \\
&= \tilde{\mathbf{A}}^{L-j-1} \frac{\exp\left(\text{softplus}(b)\mathbf{A}\right)}{1+e^{-b}} \left(\tilde{\mathbf{A}} \, \mathbf{B} u_j^3 + u_j^2 \left(\exp\left(\text{softplus}(b)\mathbf{A}\right) - \mathbf{I} \right) \mathbf{B} \sum_{i=j+1}^{L} u_i \right), \\
\mathbf{t}_j &= u_j \left(\tilde{\mathbf{A}}^{L-j} \frac{\partial}{\partial b} \mathbf{B}(u_j) + \sum_{i=j+1}^{L} \frac{\partial}{\partial b} \mathbf{A}(u_i) \tilde{\mathbf{A}}^{L-j-1} \mathbf{B}(u_j) \right) \\
&= \tilde{\mathbf{A}}^{L-j-1} \left(u_j \, \tilde{\mathbf{A}} \, \frac{\partial}{\partial b} \mathbf{B}(u_j) + u_j \left(\sum_{i=j+1}^{L} \frac{\partial}{\partial b} \mathbf{A}(u_i) \right) \mathbf{B}(u_j) \right) \\
&= \tilde{\mathbf{A}}^{L-j-1} \frac{\exp\left(\text{softplus}(b)\mathbf{A}\right)}{1+e^{-b}} \left(\tilde{\mathbf{A}} \, \mathbf{B} u_j^2 + u_j^2 (L-j) \left(\exp\left(\text{softplus}(b)\mathbf{A}\right) - \mathbf{I} \right) \mathbf{B} \right).
\end{aligned}$$

Increasing input magnitudes. From the formulas of $\mathbf{s}_j$, $\mathbf{t}_j$, and $\mathbf{r}_j$, it is straightforward that they are homogeneous in $\mathbf{u}$ with degrees 3, 2, and 1, respectively. Fixing an L, as long as $\mathbb{E}_{\mathbf{u}\sim\mathbb{D}_L}|(\partial/\partial w) y_{\text{S6}}|$, $\mathbb{E}_{\mathbf{u}\sim\mathbb{D}_L}|(\partial/\partial b) y_{\text{S6}}|$, and $\mathbb{E}_{\mathbf{u}\sim\mathbb{D}_L}|(\partial/\partial b) y_{\text{S4D}}| \neq 0$, we have that

$$\frac{\mathbb{E}_{\mathbf{u}\sim c\mathbb{D}_L}|(\partial/\partial w) y_{\text{S6}}|}{\mathbb{E}_{\mathbf{u}\sim c\mathbb{D}_L}|(\partial/\partial b) y_{\text{S4D}}|} = \mathcal{O}(c^3), \qquad \frac{\mathbb{E}_{\mathbf{u}\sim c\mathbb{D}_L}|(\partial/\partial b) y_{\text{S6}}|}{\mathbb{E}_{\mathbf{u}\sim c\mathbb{D}_L}|(\partial/\partial b) y_{\text{S4D}}|} = \mathcal{O}(c^2), \qquad c \to \infty.$$

This proves the first part of the theorem.

Increasing sequence length. The proof of the theorem when $L \to \infty$ is more involved. For clarity, we break it into three parts.

- **The gradient of y_{S4D}.** We first consider the case when $n = 1$. We will show that $\mathbb{E}_{\mathbf{u}\sim\mathbb{D}_L}|(\partial/\partial b) y_{\text{S4D}}| = \exp(b(L))\mathcal{O}(\sqrt{L})$ as $L \to \infty$. Since $\mathbf{A}$ is diagonal, when $n \geq 1$, y_{S4D} can be calculated by summing up the outputs from n independent LTI systems, all with a 1-dimensional state space. This obviously shows that $\mathbb{E}_{\mathbf{u}\sim\mathbb{D}_L}|(\partial/\partial b) y_{\text{S4D}}| = \exp(b(L))\mathcal{O}(\sqrt{L})$ when $n \geq 1$. To prove the case when $n = 1$, we use Jensen's inequality and obtain that

$$\begin{aligned}
\mathbb{E}\left[\left| \sum_{j=1}^{L} \overline{\mathbf{A}}^{L-j} \mathbf{B} u_j \right| \right] &\leq \sqrt{\mathbb{E}\left[\left| \sum_{j=1}^{L} \overline{\mathbf{A}}^{L-j} \mathbf{B} u_j \right|^2 \right]} \\
&= \sqrt{\mathbb{E}\left[\sum_{j=1}^{L} \overline{\mathbf{A}}^{L-j} \mathbf{B} u_j \right]^2 + \text{Var}\left[\sum_{j=1}^{L} \overline{\mathbf{A}}^{L-j} \mathbf{B} u_j \right]} \\
&= \sqrt{0 + \sum_{j=1}^{L} \text{Var}(v_j) + \sum_{1 \leq i < j \leq L} \text{Cov}(v_i, v_j)} = \mathcal{O}(\sqrt{L}),
\end{aligned}$$

  where $v_j = \overline{\mathbf{A}}^{L-j} \mathbf{B} u_j$. This shows that

$$\begin{aligned}
&\mathbb{E}_{\mathbf{u}\sim\mathbb{D}_L}\left[\left| \frac{\partial}{\partial b} y_{\text{S4D}} \right| \right] = \mathbb{E}_{\mathbf{u}\sim\mathbb{D}_L}\left[\left| \mathbf{C} \sum_{j=1}^{L} \mathbf{r}_j \right| \right] \\
&\leq \exp(b(L)) \left(\mathbb{E}_{\mathbf{u}\sim\mathbb{D}_L}\left[\left| \mathbf{C} \sum_{j=1}^{L} \overline{\mathbf{A}}^{L-j+1} \mathbf{B} u_j \right| \right] + \mathbb{E}_{\mathbf{u}\sim\mathbb{D}_L}\left[\left| \mathbf{C} \sum_{j=1}^{L} \overline{\mathbf{A}}^{L-j} (L-j)(\overline{\mathbf{A}} - \mathbf{I}) \mathbf{B} u_j \right| \right] \right).
\end{aligned}$$

Note that we just proved that the first expectation is $\mathcal{O}(\sqrt{L})$ as $L \to \infty$. By letting $b(L) \to -\infty$ fast enough, $\overline{\mathbf{A}} - \mathbf{I}$ vanishes exponentially, so we have the second term is also $\mathcal{O}(\sqrt{L})$. This proves that

$$\mathbb{E}_{\mathbf{u}\sim\mathbb{D}_L}|(\partial/\partial b) y_{\text{S4D}}| = \exp(b(L))\mathcal{O}(\sqrt{L}), \qquad L \to \infty. \tag{10}$$

- **The gradient of y_{S6} when $n = 1$.** When $n = 1$, the matrices $\tilde{\mathbf{A}}, \mathbf{B}$, and $\mathbf{C}$ are all scalars. Without loss of generality, assume that $\mathbf{B}, \mathbf{C} > 0$. Similar to the previous case, if $b(L) \to -\infty$ as $L \to \infty$, the matrix $\exp(\text{softplus}(b(L))\mathbf{A}) - \mathbf{I}$ vanishes. That is, since $u_L = 1$, we have

$$\mathbb{E}_{\mathbf{u}\sim\mathbb{D}_L}\left[\left|\frac{\partial}{\partial b} y_{\text{S6}}\right|\right] = \mathbb{E}_{\mathbf{u}\sim\mathbb{D}_L}\left[\left|\mathbf{C}\sum_{j=1}^{L}\mathbf{t}_j\right|\right] \sim \exp(b(L))\mathbb{E}_{\mathbf{u}\sim\mathbb{D}_L}\left[\left|\mathbf{C}\sum_{j=1}^{L}\tilde{\mathbf{A}}^{L-j}\mathbf{B}u_j^2\right|\right]$$
$$= \exp(b(L))\sum_{j=1}^{L}\mathbf{C}\tilde{\mathbf{A}}^{L-j}\mathbf{B}\,\mathbb{E}\left[u_j^2\right] \geq \exp(b(L))\sum_{j=1}^{L}\mathbf{C}\tilde{\mathbf{A}}^{L-j}\mathbf{B}\,\text{Var}\left[u_j\right] = \exp(b(L))\Theta(L),$$

provided that $b(L)$ decays fast enough so that $\tilde{\mathbf{A}}^L = \Theta(1)$ as $L \to \infty$.

- **The gradient of y_{S6} when $n > 1$.** Now, suppose $n > 1$. The output y_{S6} can be written as the sum of n terms: $y_{\text{S6}} = y_1 + \cdots + y_n$, where y_j is the output of an LTI system with $n = 1$ [97]. By the previous argument, we know that for every $1 \leq j \leq n$,

$$\mathbb{E}_{\mathbf{u}\sim\mathbb{D}_L}\left[\frac{\partial}{\partial b}\frac{y_j}{\mathbf{C}_j}\right] = \pm\exp(b(L))\Theta(L),$$

where the expectation can be either positive or negative, depending on the sign of $\mathbf{B}_j\mathbf{C}_j$. That is, we know that

$$\mathbb{E}_{\mathbf{u}\sim\mathbb{D}_L}\left[\left|\frac{\partial}{\partial b}\frac{y_j}{\mathbf{C}_j}\right|\right] \Big/ (\exp(b(L))L)$$

is bounded between two positive numbers or between two negative numbers as L is sufficiently large. We still want to apply Lemma 2 to control cancellation effects, but the main issue is that we do not have that this term converges to a number. However, since the metric space $\mathbb{R}^n$ is complete, i.e., boundedness implies subsequent convergence, we know that there exists a subsequence $L_1, L_2, \ldots$ such that

$$\mathbb{E}_{\mathbf{u}\sim\mathbb{D}_{L_k}}\left[\frac{\partial}{\partial b}\frac{y_j}{\mathbf{C}_j}\right] \to \alpha_j\exp(b(L_k))L_k \qquad \text{as} \qquad k \to \infty, \qquad 1 \leq j \leq n,$$

where α_j is a nonzero constant for all $1 \leq j \leq n$. Hence, by Lemma 2, we have for a.e. $\mathbf{C}$ that

$$\mathbb{E}_{\mathbf{u}\sim\mathbb{D}_{L_k}}\left[\frac{\partial y_{\text{S6}}}{\partial b}\right] = \mathbb{E}_{\mathbf{u}\sim\mathbb{D}_{L_k}}\left[\sum_{j=1}^{n}\frac{\partial y_j}{\partial b}\right] = \alpha\exp(b(L_k))L_k, \qquad \alpha \neq 0.$$

Hence, we have

$$\mathbb{E}_{\mathbf{u}\sim\mathbb{D}_{L_k}}\left[\left|\frac{\partial y_{\text{S6}}}{\partial b}\right|\right] = \alpha\exp(b(L_k))\Theta(L_k). \tag{11}$$

Combining eq. (10) and (11), we prove the theorem. □

E Supplementary experiments on the stability

In this section, we present two experiments to corroborate our discussion of training stability in section 5. The first experiment numerically verifies Theorem 3 as the input magnitude and the sequence length grow. The second experiment empirically shows that a reduced learning rate on Δ-related parameters help stabilize the training of an S6 model.

E.1 A numerical experiment that verifies Theorem 3

In this experiment, we set $d = 1$ and randomly sample $\text{diag}(\mathbf{A})$ from the left half of the complex plane, and randomly sample $\mathbf{B}$ and $\mathbf{C}$. We then use these matrices to construct an S4D system and an S6 system. We sample our length-L input sequences from i.i.d. Gaussian distributions with mean zero and standard deviation c.[5] We fix the ratio $L \,/\, \exp(b(L))^{-1}$ to take into account the fact that as L increases, we need a longer memory window to capture the long-range dependency. We then compute the quantities in Theorem 3. For the first two experiments, we fix $L = 100$ and let c increase. Then, we fix $c = 1$ and let L increase. The results are shown in Figure 6. All results are averaged over 30 different trials.

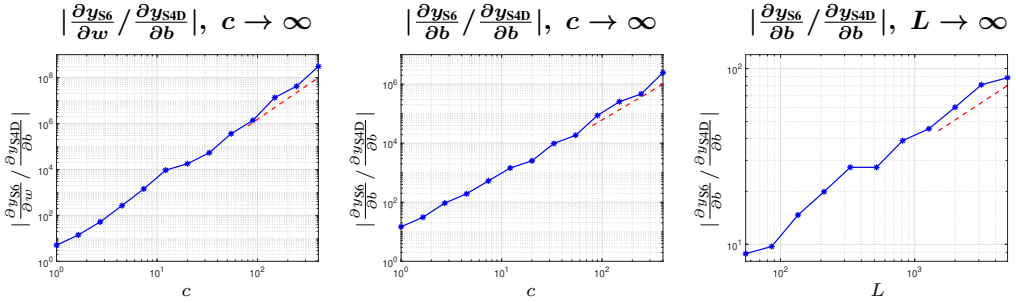

Figure 6: Numerical experiments to verify Theorem 3, where we compute the ratio between the gradients with respect to the S6 parameters and S4D parameters. For the first two figures, we fix $L = 100$; for the last figure, we fix $c = 1$. The gradients are computed using closed algebraic formulas. The red reference lines in the three log-log plots have slopes of 3, 2, and $1/2$, respectively.

In these experiments, we see that the three ratios studied in Theorem 3 follow exactly the pattern of a cubic, quadratic, and square root growth, respectively. This is what we expect from Theorem 3.

E.2 An empirical experiment on the training stability

We also show a real training example, where we want to learn a ground-truth function that takes in a univariate sequential input and returns a fixed linear combination of them: $G(u_1, \ldots, u_L) = \sum_{j=1}^{L} \theta_j u_j$, where $\theta_1, \ldots, \theta_L$ are fixed parameters. We show the loss curves in Figure 7, with different models (i.e., S4D versus S6) and different learning rate assignments (i.e., whether or not Δ is learned). We see that the S4D model is very stable during training, with its loss going down smoothly. This is not the case for the S6 model, where the loss goes up and down and even restarts. We find that by freezing the Δt parameters $\mathbf{w}$ and b, the model trains much more robustly.

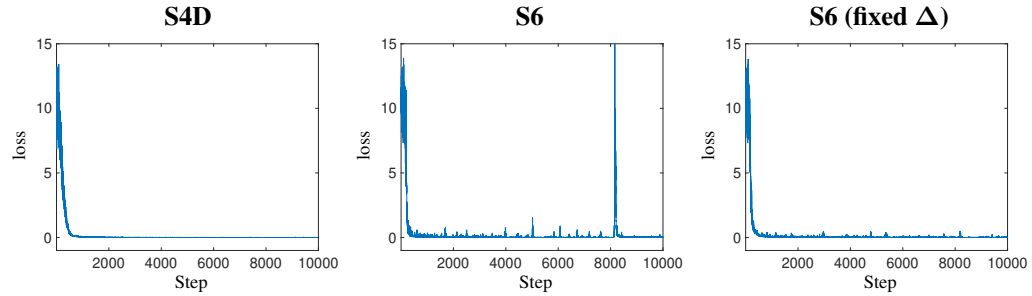

Figure 7: The root-mean-squared loss $\|G(\mathbf{u}) - \tilde{G}(\mathbf{u})\|_2$ between the true output $G(\mathbf{u})$ and the model prediction $\tilde{G(\mathbf{u})}$. The first two models are trained with a learning rate of 0.001 on the Δ parameters, whereas the last model is trained with no training of the Δ parameters.

[5] Note, in particular, that this sequence has no long-range dependency. We made this choice because it is a natural one without any prior information. It does not affect the training stability a lot. One can try different input functions with long-range dependencies, e.g., we have tried sinusoidal waves, and the results are similar.

F Details of experiments

In this section, we show the details of the experiments in section 7. Before we provide the detailed configurations, we provide an extended table for LRA results of more variants of state-space models (see Table 4). While many of these models focus on improving certain aspects of the recurrent unit, we do not incorporate and test them in our B_2S_6 model.

Table 4: An extended list of SSM accuracies on the Long-Range Arena benchmark. An entry is left blank if no result is found. All but the last three models are not input-selective.

Model	ListOps	Text	Retrieval	Image	Pathfinder	Path-X	Avg.
S4 [28]	59.60	86.82	90.90	88.65	94.20	96.35	86.09
S4D [27]	60.47	86.18	89.46	88.19	93.06	91.95	84.89
DSS [29]	57.60	76.60	87.60	85.80	84.10	85.00	79.45
LRU [55]	89.00	60.20	89.40	89.90	95.10	94.20	86.30
S4++ [61]	57.30	86.28	84.82	82.91	80.24	-	-
HOPE-SSM [98]	62.60	89.83	91.80	88.68	95.73	98.45	87.85
S4D-FT [97]	62.75	89.76	92.45	90.89	95.89	97.84	88.26
Reg. S4D [46]	61.48	88.19	91.25	88.12	94.93	95.63	86.60
Liquid S4 [30]	62.75	89.02	91.20	89.50	94.80	96.66	87.32
RTF SSM [56]	61.59	89.72	92.04	90.51	96.11	96.32	87.71
Spectral SSM [1]	60.33	89.60	90.00	-	95.60	90.10	-
Spiking SSM [72]	60.23	80.41	88.77	88.21	93.51	94.82	84.33
S5 [77]	62.15	89.31	91.40	88.00	95.33	98.58	87.46
S6 (Mamba) [25]	38.02	82.98	72.14	69.82	69.26	67.32	66.59
S7 [79]	63.77	87.22	91.80	61.14	65.62	61.50	71.82
B_2S_6 (ours)	63.85	88.32	91.44	88.81	95.93	97.90	87.71

In this paper, all models are trained with one or more NVIDIA L40 GPUs with 48GB of memory. For the ablation study, we use a 4-layer model and we increase the number of layers for the full experiments on the LRA benchmark. We provide the details of the model and training hyperparameters used for training each LRA task in Table 5. For all experiments, we set $h = 8$ so that $p = \#\text{Features}/8$. Notably, this hyperparameter h is not carefully fine-tuned but rather picked randomly. Note that our model for training the `Path-X` tasks is smaller than the corresponding S4D model.

Table 5: Configurations of our B_2S_6 model on the LRA benchmark, where LR, BS, and WD stand for learning rate, batch size, and weight decay, respectively.

Task	Depth	#Features	Norm	Prenorm	LR	BS	Epochs	WD
ListOps	8	128	BN	False	0.008	32	120	0.03
Text	6	256	BN	True	0.01	16	40	0.05
Retrieval	6	128	BN	True	0.004	60	200	0.03
Image	6	512	LN	False	0.01	48	500	0.05
Pathfinder	6	256	BN	True	0.004	48	250	0.03
Path-X	6	128	BN	True	0.001	24	120	0.03

G Limitations and Future Work

We acknowledge (and justify) several limitations of this work, which also suggest promising directions for future research:

- The universal approximation theorems (UATs) in this paper are derived under a few simplifying assumptions — most notably, the assumption that the sampling interval Δ is fixed. This setup diverges from practical implementations, where Δ is input-dependent. However, our goal is not to prove UATs for all realistic settings, but to expose fundamental expressiveness gaps between S6 and S4D under clean conditions. Extending these results to settings with dynamic Δ remains an interesting theoretical direction. If one can show that a single-layer Mamba is not a universal

approximator even when Δ is not fixed, then that would further stress the benefit of a multi-head design in selective SSMs. Conversely, if a single-layer Mamba with dynamic Δ is a universal approximator, then an important follow-up question is if (and how) a trainable channel-specific Δ can compensate for the channel-independent $\mathbf{B}$ and $\mathbf{C}$ matrices in a single-head Mamba.

- Our experiments on language modeling are not designed to compete with large-scale models or datasets. This choice reflects a deliberate focus: our primary aim is to study and improve the behavior of Mamba on long-range sequence tasks. Demonstrating that $\mathrm{B}_2\mathrm{S}_6$ retains Mamba's performance in language modeling — even at small scale — supports its versatility. Scaling to larger models and corpora is a natural next step, pending access to greater computational resources.
- Our implementation of $\mathrm{B}_2\mathrm{S}_6$ is based entirely on PyTorch. While this makes the method easily accessible and reproducible, further speed improvements would require low-level optimization in CUDA (see [25]). We leave efficient implementation and integration into high-performance inference/training libraries to future work.

NeurIPS Paper Checklist

1. **Claims**

   Question: Do the main claims made in the abstract and introduction accurately reflect the paper's contributions and scope?

   Answer: [Yes]

   Justification: The abstract and the introduction clearly state the main claims and contributions of the paper. It is made clear that the paper focuses on investigating Mamba's capability of modeling long-range sequences, and that the paper analyzes the previous limitations from three aspects (expressiveness, inductive bias, and training stability) and proposes a model that better captures long-range dependencies. All claims are supported by both theoretical statements and experiments.

   Guidelines:

   - The answer NA means that the abstract and introduction do not include the claims made in the paper.
   - The abstract and/or introduction should clearly state the claims made, including the contributions made in the paper and important assumptions and limitations. A No or NA answer to this question will not be perceived well by the reviewers.
   - The claims made should match theoretical and experimental results, and reflect how much the results can be expected to generalize to other settings.
   - It is fine to include aspirational goals as motivation as long as it is clear that these goals are not attained by the paper.

2. **Limitations**

   Question: Does the paper discuss the limitations of the work performed by the authors?

   Answer: [Yes]

   Justification: We discuss the limitations of this paper in Appendix G. These limitations are also discussed in the main paper, though not in a centralized way.

   Guidelines:

   - The answer NA means that the paper has no limitation while the answer No means that the paper has limitations, but those are not discussed in the paper.
   - The authors are encouraged to create a separate "Limitations" section in their paper.
   - The paper should point out any strong assumptions and how robust the results are to violations of these assumptions (e.g., independence assumptions, noiseless settings, model well-specification, asymptotic approximations only holding locally). The authors should reflect on how these assumptions might be violated in practice and what the implications would be.
   - The authors should reflect on the scope of the claims made, e.g., if the approach was only tested on a few datasets or with a few runs. In general, empirical results often depend on implicit assumptions, which should be articulated.
   - The authors should reflect on the factors that influence the performance of the approach. For example, a facial recognition algorithm may perform poorly when image resolution is low or images are taken in low lighting. Or a speech-to-text system might not be used reliably to provide closed captions for online lectures because it fails to handle technical jargon.
   - The authors should discuss the computational efficiency of the proposed algorithms and how they scale with dataset size.
   - If applicable, the authors should discuss possible limitations of their approach to address problems of privacy and fairness.
   - While the authors might fear that complete honesty about limitations might be used by reviewers as grounds for rejection, a worse outcome might be that reviewers discover limitations that aren't acknowledged in the paper. The authors should use their best judgment and recognize that individual actions in favor of transparency play an important role in developing norms that preserve the integrity of the community. Reviewers will be specifically instructed to not penalize honesty concerning limitations.

3. **Theory assumptions and proofs**

   Question: For each theoretical result, does the paper provide the full set of assumptions and a complete (and correct) proof?

   Answer: [Yes]

   Justification: All assumptions are clearly stated, with notations previously defined in the paper clearly cross-referenced. All proofs are provided in the appendices.

   Guidelines:

   - The answer NA means that the paper does not include theoretical results.
   - All the theorems, formulas, and proofs in the paper should be numbered and cross-referenced.
   - All assumptions should be clearly stated or referenced in the statement of any theorems.
   - The proofs can either appear in the main paper or the supplemental material, but if they appear in the supplemental material, the authors are encouraged to provide a short proof sketch to provide intuition.
   - Inversely, any informal proof provided in the core of the paper should be complemented by formal proofs provided in appendix or supplemental material.
   - Theorems and Lemmas that the proof relies upon should be properly referenced.

4. **Experimental result reproducibility**

   Question: Does the paper fully disclose all the information needed to reproduce the main experimental results of the paper to the extent that it affects the main claims and/or conclusions of the paper (regardless of whether the code and data are provided or not)?

   Answer: [Yes]

   Justification: We provide details of all experiments in Appendix F. While it is infeasible to state all details of the training and model configurations, we provide anonymous code to enhance the reproducibility of the experiments.

   Guidelines:

   - The answer NA means that the paper does not include experiments.
   - If the paper includes experiments, a No answer to this question will not be perceived well by the reviewers: Making the paper reproducible is important, regardless of whether the code and data are provided or not.
   - If the contribution is a dataset and/or model, the authors should describe the steps taken to make their results reproducible or verifiable.
   - Depending on the contribution, reproducibility can be accomplished in various ways. For example, if the contribution is a novel architecture, describing the architecture fully might suffice, or if the contribution is a specific model and empirical evaluation, it may be necessary to either make it possible for others to replicate the model with the same dataset, or provide access to the model. In general. releasing code and data is often one good way to accomplish this, but reproducibility can also be provided via detailed instructions for how to replicate the results, access to a hosted model (e.g., in the case of a large language model), releasing of a model checkpoint, or other means that are appropriate to the research performed.
   - While NeurIPS does not require releasing code, the conference does require all submissions to provide some reasonable avenue for reproducibility, which may depend on the nature of the contribution. For example
     (a) If the contribution is primarily a new algorithm, the paper should make it clear how to reproduce that algorithm.
     (b) If the contribution is primarily a new model architecture, the paper should describe the architecture clearly and fully.
     (c) If the contribution is a new model (e.g., a large language model), then there should either be a way to access this model for reproducing the results or a way to reproduce the model (e.g., with an open-source dataset or instructions for how to construct the dataset).

(d) We recognize that reproducibility may be tricky in some cases, in which case authors are welcome to describe the particular way they provide for reproducibility. In the case of closed-source models, it may be that access to the model is limited in some way (e.g., to registered users), but it should be possible for other researchers to have some path to reproducing or verifying the results.

5. **Open access to data and code**

   Question: Does the paper provide open access to the data and code, with sufficient instructions to faithfully reproduce the main experimental results, as described in supplemental material?

   Answer: [Yes]

   Justification: We provide anonymous code with our submission. They come along with clear instructions, allowing for faithful reproducibility. The datasets are external and instructions are given to download them.

   Guidelines:

   - The answer NA means that paper does not include experiments requiring code.
   - Please see the NeurIPS code and data submission guidelines (`https://nips.cc/public/guides/CodeSubmissionPolicy`) for more details.
   - While we encourage the release of code and data, we understand that this might not be possible, so "No" is an acceptable answer. Papers cannot be rejected simply for not including code, unless this is central to the contribution (e.g., for a new open-source benchmark).
   - The instructions should contain the exact command and environment needed to run to reproduce the results. See the NeurIPS code and data submission guidelines (`https://nips.cc/public/guides/CodeSubmissionPolicy`) for more details.
   - The authors should provide instructions on data access and preparation, including how to access the raw data, preprocessed data, intermediate data, and generated data, etc.
   - The authors should provide scripts to reproduce all experimental results for the new proposed method and baselines. If only a subset of experiments are reproducible, they should state which ones are omitted from the script and why.
   - At submission time, to preserve anonymity, the authors should release anonymized versions (if applicable).
   - Providing as much information as possible in supplemental material (appended to the paper) is recommended, but including URLs to data and code is permitted.

6. **Experimental setting/details**

   Question: Does the paper specify all the training and test details (e.g., data splits, hyperparameters, how they were chosen, type of optimizer, etc.) necessary to understand the results?

   Answer: [Yes]

   Justification: We provide the table of hyperparameters in Appendix F. While we do not specify all training and test details, including the data splits and optimizers, most of the experiments come with standard choices, and they can be found in our anonymous code repository.

   Guidelines:

   - The answer NA means that the paper does not include experiments.
   - The experimental setting should be presented in the core of the paper to a level of detail that is necessary to appreciate the results and make sense of them.
   - The full details can be provided either with the code, in appendix, or as supplemental material.

7. **Experiment statistical significance**

   Question: Does the paper report error bars suitably and correctly defined or other appropriate information about the statistical significance of the experiments?

   Answer: [Yes]

Justification: We repeat our ablation study and Long-Range Arena experiments with multiple random seeds and report the standard deviations in section 7.

Guidelines:

- The answer NA means that the paper does not include experiments.
- The authors should answer "Yes" if the results are accompanied by error bars, confidence intervals, or statistical significance tests, at least for the experiments that support the main claims of the paper.
- The factors of variability that the error bars are capturing should be clearly stated (for example, train/test split, initialization, random drawing of some parameter, or overall run with given experimental conditions).
- The method for calculating the error bars should be explained (closed form formula, call to a library function, bootstrap, etc.)
- The assumptions made should be given (e.g., Normally distributed errors).
- It should be clear whether the error bar is the standard deviation or the standard error of the mean.
- It is OK to report 1-sigma error bars, but one should state it. The authors should preferably report a 2-sigma error bar than state that they have a 96% CI, if the hypothesis of Normality of errors is not verified.
- For asymmetric distributions, the authors should be careful not to show in tables or figures symmetric error bars that would yield results that are out of range (e.g. negative error rates).
- If error bars are reported in tables or plots, The authors should explain in the text how they were calculated and reference the corresponding figures or tables in the text.

8. **Experiments compute resources**

   Question: For each experiment, does the paper provide sufficient information on the computer resources (type of compute workers, memory, time of execution) needed to reproduce the experiments?

   Answer: [Yes]

   Justification: Details of the compute resources are given in Appendix F. We do not measure the time of execution of the Long-Range Arena experiments as they are not standardly reported in the state-space models community.

   Guidelines:

   - The answer NA means that the paper does not include experiments.
   - The paper should indicate the type of compute workers CPU or GPU, internal cluster, or cloud provider, including relevant memory and storage.
   - The paper should provide the amount of compute required for each of the individual experimental runs as well as estimate the total compute.
   - The paper should disclose whether the full research project required more compute than the experiments reported in the paper (e.g., preliminary or failed experiments that didn't make it into the paper).

9. **Code of ethics**

   Question: Does the research conducted in the paper conform, in every respect, with the NeurIPS Code of Ethics `https://neurips.cc/public/EthicsGuidelines`?

   Answer: [Yes]

   Justification: The work complies with the Code of Ethics.

   Guidelines:

   - The answer NA means that the authors have not reviewed the NeurIPS Code of Ethics.
   - If the authors answer No, they should explain the special circumstances that require a deviation from the Code of Ethics.
   - The authors should make sure to preserve anonymity (e.g., if there is a special consideration due to laws or regulations in their jurisdiction).

10. **Broader impacts**

Question: Does the paper discuss both potential positive societal impacts and negative societal impacts of the work performed?

Answer: [NA]

Justification: This work is theoretical and methodological. It does not involve large-scale implementation and experimentation and has very limited societal impact.

Guidelines:

- The answer NA means that there is no societal impact of the work performed.
- If the authors answer NA or No, they should explain why their work has no societal impact or why the paper does not address societal impact.
- Examples of negative societal impacts include potential malicious or unintended uses (e.g., disinformation, generating fake profiles, surveillance), fairness considerations (e.g., deployment of technologies that could make decisions that unfairly impact specific groups), privacy considerations, and security considerations.
- The conference expects that many papers will be foundational research and not tied to particular applications, let alone deployments. However, if there is a direct path to any negative applications, the authors should point it out. For example, it is legitimate to point out that an improvement in the quality of generative models could be used to generate deepfakes for disinformation. On the other hand, it is not needed to point out that a generic algorithm for optimizing neural networks could enable people to train models that generate Deepfakes faster.
- The authors should consider possible harms that could arise when the technology is being used as intended and functioning correctly, harms that could arise when the technology is being used as intended but gives incorrect results, and harms following from (intentional or unintentional) misuse of the technology.
- If there are negative societal impacts, the authors could also discuss possible mitigation strategies (e.g., gated release of models, providing defenses in addition to attacks, mechanisms for monitoring misuse, mechanisms to monitor how a system learns from feedback over time, improving the efficiency and accessibility of ML).

11. **Safeguards**

Question: Does the paper describe safeguards that have been put in place for responsible release of data or models that have a high risk for misuse (e.g., pretrained language models, image generators, or scraped datasets)?

Answer: [NA]

Justification: The paper releases no data or models that have a high risk of misuse.

Guidelines:

- The answer NA means that the paper poses no such risks.
- Released models that have a high risk for misuse or dual-use should be released with necessary safeguards to allow for controlled use of the model, for example by requiring that users adhere to usage guidelines or restrictions to access the model or implementing safety filters.
- Datasets that have been scraped from the Internet could pose safety risks. The authors should describe how they avoided releasing unsafe images.
- We recognize that providing effective safeguards is challenging, and many papers do not require this, but we encourage authors to take this into account and make a best faith effort.

12. **Licenses for existing assets**

Question: Are the creators or original owners of assets (e.g., code, data, models), used in the paper, properly credited and are the license and terms of use explicitly mentioned and properly respected?

Answer: [Yes]

Justification: The existing assets are both acknowledged in Appendix F and the anonymous code repository.

Guidelines:

- The answer NA means that the paper does not use existing assets.
- The authors should cite the original paper that produced the code package or dataset.
- The authors should state which version of the asset is used and, if possible, include a URL.
- The name of the license (e.g., CC-BY 4.0) should be included for each asset.
- For scraped data from a particular source (e.g., website), the copyright and terms of service of that source should be provided.
- If assets are released, the license, copyright information, and terms of use in the package should be provided. For popular datasets, `paperswithcode.com/datasets` has curated licenses for some datasets. Their licensing guide can help determine the license of a dataset.
- For existing datasets that are re-packaged, both the original license and the license of the derived asset (if it has changed) should be provided.
- If this information is not available online, the authors are encouraged to reach out to the asset's creators.

13. **New assets**

    Question: Are new assets introduced in the paper well documented and is the documentation provided alongside the assets?

    Answer: [Yes]

    Justification: The anonymous code repository we provide is well-documented and contains a README file that explains the organization of the repository and steps needed to reproduce our experimental results.

    Guidelines:

    - The answer NA means that the paper does not release new assets.
    - Researchers should communicate the details of the dataset/code/model as part of their submissions via structured templates. This includes details about training, license, limitations, etc.
    - The paper should discuss whether and how consent was obtained from people whose asset is used.
    - At submission time, remember to anonymize your assets (if applicable). You can either create an anonymized URL or include an anonymized zip file.

14. **Crowdsourcing and research with human subjects**

    Question: For crowdsourcing experiments and research with human subjects, does the paper include the full text of instructions given to participants and screenshots, if applicable, as well as details about compensation (if any)?

    Answer: [NA]

    Justification: This paper does not involve crowdsourcing.

    Guidelines:

    - The answer NA means that the paper does not involve crowdsourcing nor research with human subjects.
    - Including this information in the supplemental material is fine, but if the main contribution of the paper involves human subjects, then as much detail as possible should be included in the main paper.
    - According to the NeurIPS Code of Ethics, workers involved in data collection, curation, or other labor should be paid at least the minimum wage in the country of the data collector.

15. **Institutional review board (IRB) approvals or equivalent for research with human subjects**

    Question: Does the paper describe potential risks incurred by study participants, whether such risks were disclosed to the subjects, and whether Institutional Review Board (IRB) approvals (or an equivalent approval/review based on the requirements of your country or institution) were obtained?

Answer: [NA]

Justification: This paper does not involve crowdsourcing nor research with human subjects.

Guidelines:

- The answer NA means that the paper does not involve crowdsourcing nor research with human subjects.
- Depending on the country in which research is conducted, IRB approval (or equivalent) may be required for any human subjects research. If you obtained IRB approval, you should clearly state this in the paper.
- We recognize that the procedures for this may vary significantly between institutions and locations, and we expect authors to adhere to the NeurIPS Code of Ethics and the guidelines for their institution.
- For initial submissions, do not include any information that would break anonymity (if applicable), such as the institution conducting the review.

16. **Declaration of LLM usage**

Question: Does the paper describe the usage of LLMs if it is an important, original, or non-standard component of the core methods in this research? Note that if the LLM is used only for writing, editing, or formatting purposes and does not impact the core methodology, scientific rigorousness, or originality of the research, declaration is not required.

Answer: [NA]

Justification: LLMs are only used for word choices and limited polishing of the writing. This research does not involve LLMs as any important, original, or non-standard components.

Guidelines:

- The answer NA means that the core method development in this research does not involve LLMs as any important, original, or non-standard components.
- Please refer to our LLM policy (`https://neurips.cc/Conferences/2025/LLM`) for what should or should not be described.